Published in final edited form as:

Brain Behav Immun. 2021 March ; 93: 141–155. doi:10.1016/j.bbi.2020.12.034.

Regulation of post-ischemic inflammatory response: A novel function of the neuronal tyrosine phosphatase STEP

Sathyanarayanan Rajagopal[a], **Changjun Yang**[c], **Kelly M. DeMars**[c], **Ranjana Poddar**[a], **Eduardo Candelario-Jalil**[c], **Surojit Paul**[a,b,*]

[a]University of New Mexico Health Sciences Center, Department of Neurology, USA

[b]University of New Mexico Health Sciences Center, Department of Neuroscience, USA

[c]University of Florida, Department of Neuroscience, USA

Abstract

The neuron-specific tyrosine phosphatase STEP is emerging as a key neuroprotectant against acute ischemic stroke. However, it remains unclear how STEP impacts the outcome of stroke. We find that the exacerbation of ischemic brain injury in STEP deficient mice involves an early onset and sustained activation of neuronal p38 mitogen activated protein kinase, a substrate of STEP. This leads to rapid increase in the expression of neuronal cyclooxygenase-2 and synthesis of prostaglandin E_2, causing change in microglial morphology to an amoeboid activated state, activation of matrix metalloproteinase-9, cleavage of tight junction proteins and extravasation of IgG into the ischemic brain. Restoration of STEP signaling with intravenous administration of a STEP-derived peptide mimetic reduces the post-ischemic inflammatory response and attenuates brain injury. The findings identify a unique role of STEP in regulating post-ischemic neuroinflammation and further emphasizes the therapeutic potential of the STEP-mimetic in neurological disorders where inflammation contributes to brain damage.

Keywords

Tyrosine phosphatase; STEP; Cerebral ischemia; Inflammation; p38 MAP kinase; Cyclooxygenase-2; Prostaglandin E_2; Neuroprotection

1. Introduction

Ischemic stroke is a leading cause of death and disability worldwide. Despite advances in understanding the pathophysiology of acute ischemic stroke, effective treatments to minimize damage and improve recovery are still unavailable. Evidence from a large number of studies suggests that activation of glutamate receptors, particularly the N-methyl-D-aspartate subtype (NMDARs), plays a central role in initiation and progression of ischemic

*Corresponding author. Address: University of New Mexico Health Sciences Center, Department of Neurology, 1 University of New Mexico, Albuquerque, NM 87131, USA. spaul@salud.unm.edu, (S. Paul).

Declaration of Competing Interest

The authors declare that they have no known competing financial interests or personal relationships that could have appeared to influence the work reported in this paper.

brain damage (Arundine and Tymianski, 2004; Lau and Tymianski, 2010; Liu et al., 2007). However, neuroprotective agents that have targeted NMDARs have failed in clinical trials, as inhibition of physiological functions of NMDARs, required for normal synaptic plasticity and recovery, may have contributed to neuropsychological side effects and lack of efficacy (Hoyte et al., 2004; Ikonomidou and Turski, 2002). Several recent studies have suggested that this difficulty can potentially be overcome by targeting the excitotoxic signaling cascade downstream of NMDAR stimulation (Hoque et al., 2016).

Emerging evidence indicate that the brain-enriched and neuron-specific tyrosine phosphatase STEP (striatal enriched tyrosine phosphatase, also known as Ptpn5), a signaling molecule downstream of NMDAR stimulation, is a key regulator of neuronal survival and death (Boulanger et al., 1995; Lombroso et al., 1993; Paul and Connor, 2010; Paul et al., 2003, 2000; Poddar et al., 2010). In cell culture models of excitotoxicity and oxygen glucose deprivation, dephosphorylation and subsequent activation of STEP has been shown to contribute to neuroprotection (Deb et al., 2013; Poddar et al., 2010). Using a rat model of transient focal ischemia, it has also been shown that rapid activation of STEP during the ischemic insult provides initial neuroprotection, while degradation of active STEP over time leads to secondary activation of deleterious processes, resulting in progression of ischemic brain damage (Deb et al., 2013). Another potentially important finding is that STEP activity decreases with aging (Rajagopal et al., 2016), suggesting that the loss of this protective response may be a contributing factor for the increased susceptibility of the aging brain to ischemic brain damage (Howard et al., 1987; Nakayama et al., 1994). Consistent with this interpretation, studies in STEP knockout (KO) mice further showed that loss of endogenous STEP leads to exacerbation of ischemic brain injury as observed 24 h after a mild ischemic insult. The findings also showed that ischemic insult in the absence of STEP leads to increase in phosphorylation of p38 MAPK, a substrate of STEP that has been implicated in ischemic brain injury (Deb et al., 2013; Poddar et al., 2010). Based on these observations additional studies developed a brain-permeable STEP-derived peptide mimetic that is resistant to degradation (TAT-STEP-Myc), and showed that it is effective in limiting acute stroke injury and facilitates long-term recovery in a rat model of stroke, even when administered 6 h after the onset of an insult (Deb et al., 2013). Studies in STEP KO mice further showed that restoration of the STEP signaling pathway with the administration of the peptide mimetic could also attenuate the exacerbation of ischemic brain injury in the absence of endogenous STEP (Deb et al., 2013). These findings highlight the importance of STEP in neuroprotection against ischemic brain injury. However, the molecular basis of this neuroprotection is not fully understood. To address this issue in the present study we utilized the STEP KO mice as a tool to identify the signaling cascade regulated by STEP to limit ischemic brain damage. Our findings show that STEP is a key regulator of post-ischemic inflammatory response in the brain.

Both experimental and clinical studies have highlighted the role of post-ischemic inflammation, characterized by microglial activation, in the progression of brain damage after stroke; however, the cellular mechanisms and the cell types that are involved in triggering post-ischemic inflammation are not fully understood. Here we present data that identifies STEP as a key regulator of neuronal release of the pro-inflammatory mediator prostaglandin E_2 (PGE_2), which accelerates microglial activation, BBB damage and

peripheral immune cell infiltration resulting in exacerbation of ischemic brain damage. To the best of our knowledge no study has yet identified the role of a tyrosine phosphatase as a determinant of neuroinflammatory response and severity of the ischemic brain injury.

2. Materials and methods

2.1. Experimental model

STEP knockout mice (KO or $STEP^{-/-}$) were developed on a C57BL6 background (Venkitaramani et al., 2009) and were obtained as a gift from Dr. Paul J Lombroso (Yale University). Breeding pairs of mice with heterozygous deletion of the STEP gene were used to generate both WT and STEP KO mice at the University of New Mexico Animal Care Facility. The mice were maintained in a 12-h light/dark vivarium (light off at 18.00 h) and with access to food and water ad libitum in our animal facility. The study utilized male WT mice (n = 78) and STEP KO mice (n = 104) that were 12–14 weeks old (26–27 g). For all the experiments WT and STEP KO mice were randomly assigned for sham surgery, middle cerebral artery occlusion (MCAO) or MCAO with peptide treatment (TAT-STEP-myc). Biochemical studies evaluated the temporal profile of p38 MAPK phosphorylation, COX-2 expression and PGE_2 level at different time points after stroke and reperfusion in both WT and STEP KO mice (n = 3–5/group/time point). Subsequent studies assessed the efficacy of treatment with a STEP peptide mimetic (TAT-STEP-myc) in attenuating p38 MAPK phosphorylation, COX-2 expression and PGE_2 synthesis (n = 3–6 mice/group). The next set of experiments determined the effect of stroke on the activation of MMP-9, degradation of tight junction proteins and extravasation of immunoglobulins (IgG), as well as the efficacy of treatment with STEP-peptide mimetic (n = 7–12 mice/group). Additional experiments evaluated post-stroke neurological and motor deficits in STEP KO mice and the efficacy of peptide treatment on these functional outcomes (n = 4–7 mice/group). Fluoro-jade and immunohistochemical staining were also carried out to assess post-stroke infarct size and microglial activation (n = 3–5 mice/group). All procedures involving animal follow the ARRIVE guidelines and approved by the University of New Mexico, Health Sciences Center, Institutional Animal Care and Use Committee.

2.2. Construction and purification of the STEP-derived peptide TAT-STEP-Myc

A recombinant DNA construct for TAT-STEP-Myc peptide was generated using a bacterial expression vector, expressed in *E. Coli* and purified as described previously (Paul et al., 2003). Briefly, $STEP_{61}$ cDNA lacking the PTP domain and encoding only 173–279 amino acids was sub-cloned into a pTrc-His-Myc-TOPO expression vector (Invitrogen). A 11 amino acid TAT peptide (*trans*-activator of transcription of human immunodeficiency virus) nucleotide sequence was inserted at the N-terminal of the STEP ΔPTP cDNA to render the peptide cell permeable (Poddar et al., 2010). A point mutation was introduced by site-directed mutagenesis (Pfu Turbo, Stratagene) at serine 221 within the KIM domain (S221A) to render the peptide constitutively active in terms of its ability to bind to its substrate. Point mutations were also introduced at threonine 231 (T231E) and serine 244 (S244E) in the KIS domain to mimic the phosphorylated form that helps to maintain the stability of STEP (Mukherjee et al., 2011). The modified TAT-STEP-Myc peptide was expressed in *E. Coli* and purified using BD-Talon resin (BD Biosciences, Bedford, MA, USA).

2.3. Induction of transient focal cerebral ischemia

MCAO was performed on male WT and STEP KO mice using the intraluminal method as described earlier (Deb et al., 2013; Longa et al., 1989) by a blinded experimenter. Briefly, animals were anesthetized by spontaneous inhalation of isoflurane (2%) in 70% nitrous oxide and 30% oxygen. Rectal temperature was maintained at 37 ± 1 °C with an electrical heating pad both during surgery and recovery. The right common carotid artery (CCA) and the external carotid artery were exposed by a ventral midline incision in the neck region and clipped. Both the external carotid artery and pterygopalatine branch of the internal carotid artery were clipped to allow proper insertion of the occluding filament. A silicon-rubber-coated 6–0 monofilament (Doccol Corporation) was advanced through the CCA into the internal carotid artery to a length of 10–11 mm from the bifurcation to occlude the middle cerebral artery. Depending on the experiment, the occluding filament was kept in place for 10–30 min or the filament was retracted after 30 min of occlusion to allow reperfusion for various durations (3 h–24 h). For reperfusion, the incision was closed under anesthesia and animals were allowed to recover in their cages. In some experiments, STEP KO mice received a single intravenous dose of TAT-STEP-Myc peptide (3 nmol/g of body weight) through the femoral vein at the onset of reperfusion (Deb et al., 2013; Poddar et al., 2019). At the specified time points after occlusion or reperfusion WT and STEP KO mice were euthanized and used for biochemical studies, immunohistochemistry or Fluoro-Jade C staining.

2.4. Immunoblotting

For immunoblotting studies mice were decapitated after sham surgery and at specified time points after MCAO (10 and 30 min) and reperfusion (3, 6 and 24 h). Brain slices (2 mm thickness) were obtained using the coronal mouse brain mold. Cortical and striatal tissue punches from the third rostral section of ipsilateral hemispheres were homogenized in Laemmli sample buffer, boiled at 100 °C for 10 min, centrifuged at 14,000 × g (10 min) and equal amount of protein (estimated using BCA kit, Pierce) from the supernatant was processed for SDS-PAGE and immunoblotting (Deb et al., 2013) with the following primary antibodies against proteins of interest: polyclonal anti-p38 (1:1000, Cat # 9218) and rabbit monoclonal anti-phospho-p38 ($T^{P}EY^{P}$) from Cell Signaling (Cat #: 9215); polyclonal anti-cyclooxygenase-2 (COX-2) from Abcam (Cat #: ab15191); monoclonal anti-β-tubulin from Sigma Aldrich (Cat #: T0198); monoclonal anti-STEP from Novus Biologicals (Cat #: NB300–202); polyclonal anti-zona occluden-1 (ZO-1) from Thermo Fisher (Cat #: 61–7300); and rabbit monoclonal anti-occludin from Abcam (Cat #: ab167161). Horseradish peroxidase conjugated goat anti-rabbit (1:1000–2000, Cat #: 7074) or goat anti-mouse (1:2000, Cat #: 7076) from Cell Signaling was used as secondary antibody. Additional information on the above antibodies are listed in Table 1. Immune complexes were detected on X-ray film after treatment with West Pico super signal chemiluminescence reagent (Pierce Biotechnology). Quantification of phosphorylated p38 MAPK, COX-2, ZO-1 and Occludin-125 was done by computer-assisted densitometry and Image J analysis as described earlier (Deb et al., 2013; Poddar et al., 2016).

2.5. Enzyme linked immunoassay for prostaglandin E_2

To determine prostaglandin E_2 (PGE_2) concentrations, WT and STEP KO mice were subjected to MCAO for 30 min followed by reperfusion for 6 h. The 6 h time point was chosen to compare the effect of transient increase in COX-2 expression in WT mice at 6 h after reperfusion with the sustained increase in COX-2 expression in the STEP KO mice after reperfusion. Mice were euthanized after sham surgery and 6 h after post-MCAO reperfusion, and brains were rapidly removed on ice. Cortex and striatum were dissected out from the third rostral section of coronal brain slices (2 mm thickness) obtained from ipsilateral hemisphere. The tissues were homogenized separately in ice cold PBS in the presence of protease inhibitor cocktail (Roche), centrifuged at 14,000 rpm for 10 min. The supernatant was removed and equal amount of protein in each sample was estimated using BCA protein estimation kit (Pierce). Equal amount of protein from each sample (10 μg) was used for PGE_2 assay using the PGE_2 enzyme immunoassay kit (K051-H1) from Arbor assays (Ann Arbor, MI) according to the manufacturer's protocol. Briefly, the assay was performed in a microtiter plate coated with goat-anti-mouse IgG to capture a mouse monoclonal antibody specific for PGE_2. The reaction was initiated following addition of a fixed amount of sample (or standard PGE_2), HRP-conjugated PGE_2 and the antibody against PGE_2 to the well. The assay is based on a competitive binding technique in which PGE_2 present in the sample competes with the HRP-conjugated PGE_2 for sites on the bound mouse monoclonal antibody. After a 2 h incubation with shaking at room temperature and a brief washing to remove unbound sample and excess HRP-conjugated PGE_2, a substrate solution was added to the wells to determine the enzyme activity of the bound HRP-conjugated PGE_2. The intensity of the color, measured at 450 nm wavelength is inversely proportional to the concentration of PGE_2 in the sample.

2.6. Enzyme linked immunoassay for detection of IgG in brain

To determine immunoglobulin G (IgG) level in the brain as a measure of blood–brain barrier (BBB) permeability, WT and STEP KO mice were subjected to MCAO for 30 min followed by reperfusion for 24 h. Mice were rapidly decapitated after sham surgery and 24 h after post-MCAO reperfusion, brains were removed and cortical and striatal lysates from the ipsilateral hemisphere were obtained as described above. The tissue was homogenized separately in RIPA buffer containing 1% SDS, 1% sodium deoxycholate, 150 mM NaCl, 50 mM Tris-HCl pH 7.6, and 1% IGEPAL CA-630 (Sigma-Aldrich) at 10 μL/mg of brain tissue. HALT Protease Inhibitor Cocktail, HALT Phosphatase Inhibitor Cocktail and 0.5 M EDTA were added at 10 μL/mL of homogenization buffer immediately before use. Homogenates were spun down at 14,000 × g at 4 °C for 20 min and supernatant was removed and stored at −80 °C until analysis. An amount of 50 μg of total of protein from each sample was used for determination of IgG levels using a mouse IgG ELISA kit (E-90G) from Immunology Consultants Laboratory, Inc. following the manufacturer's protocol.

2.7. Fluorometric immunocapture assay for MMP-9 activity

Enzymatic activity of MMP-9 in the ipsilateral cortex and striatum of WT and STEP KO mice subjected to 18 h reperfusion after MCAO was measured using a fluorescence resonance energy transfer (FRET) peptide immunoassay as described earlier (Hawkins et al.,

2013). Briefly, high binding 96 well plates were first coated with protein A/G (200 μg/ml; ScienCell, Carlsbad, CA) in a carbonate/bicarbonate buffer (pH 9.4) for 2 h at room temperature. After washing the wells three times with TCNB buffer (200 μL each time, 50 mM Tris-HCl, 10 mM $CaCl_2$, 150 mM NaCl, 0.05% Brij L23) 0.5 μg of polyclonal rabbit anti-MMP-9 antibody (Cat. No. SC-6841-R, Santa Cruz Biotechnology) was added to each well and incubated for another 2 h. The wells were then washed again with TCNB buffer (three times) followed by addition of 50 μg of cortical and striatal lysates obtained from the ipsilateral hemisphere of WT and STEP KO mice and incubated overnight at 4 °C. After washing with TCNB buffer 5- FAM/QXL™ 520 FRET peptide substrate (Substrate III Cat. No. AS-60570–01, Anaspec, Fremont, CA) was added to the wells. The plates were then incubated at 37 °C for 24 h, and then read at excitation/emission wavelengths of 485/528 nm in a Synergy HT multi-mode microplate fluorescence reader. Basal fluorescence was measured from wells where tissue lysates were not added and subtracted from the fluorescence values obtained from the sample treated wells to provide the final relative fluorescent unit (RFU) value for each sample.

2.8. Immunohistochemistry and quantification of Iba-1 fluorescence intensity

Six hours after MCAO/reperfusion mice were rapidly anesthetized and perfused intracardially with ice-cold 4% paraformaldehyde in 0.01 M PBS. Brains were then removed and post-fixed in the same fixative solution for 4 h and cryoprotected in 15% and 30% sucrose in PBS and then frozen in Optical Cutting Temperature (OCT) compound. Brains were removed, cryoprotected and frozen for cryosectioning. Immunohistochemistry with rabbit monoclonal anti-phospho-p38 ($T^{P}EY^{P}$) (Cat # 4631), polyclonal anti-COX-2 (1:100); monoclonal anti-NeuN antibody from EMD Millipore (Cat # MAB-377); and polyclonal anti-Iba-1 antibody from Wako (Cat # 019–19741) were performed on 16 μm sections. Briefly, coronal sections through the cortex were blocked with 10% normal goat serum, 3% BSA in PBS-T (PBS with 0.2% Triton X-100) for 1 h at room temperature and incubated overnight with the respective primary antibody. After extensive washing with PBS-T, sections were incubated with AlexaFluor-488 conjugated goat anti-rabbit antibody from Thermo Fisher (Cat #: A11008), AlexaFluor-488 conjugated goat anti-mouse antibody Thermo Fisher (Cat #: A11001) or Cy3 conjugated goat anti-rabbit antibody from Jackson Immuno-Research Laboratories (Cat # 111–165-144) for 1 h at room temperature. Sections were washed three times in PBS-T and mounted using ProLong Gold Antifade mounting media. All sections were imaged using fluorescent microscopy (Olympus IX-71). To quantify microglial activation ImageJ (National Institutes of Health, Bethesda, MD, USA) was used to measure immunofluorescent staining intensity of Iba-1 in images captured from ischemic hemisphere of WT and STEP KO mice brain. Since Iba-1 is specifically expressed in microglia in the brain and is upregulated during the activation of these cells, increased intensity of Iba-1 immunofluorescence represents microgliosis (Ito et al., 2001; Patel et al., 2013; Yang et al., 2015). Additional details on the above antibodies are listed in Table 1.

2.9. Fluoro-Jade C staining and infarct volume measurement

At the specified time points after MCAO (6, 12 and 24 h after reperfusion) or following sham surgery mice were anesthetized with sodium pentobarbital (150 mg/kg, i.p.) and perfused intracardially as described above and then frozen in OCT compound. Coronal

forebrain sections were collected at 90 μm intervals. For Fluoro-Jade C staining sections were air-dried, dehydrated, incubated with 0.06% potassium permanganate (15 min), rinsed in water and stained with 0.001% Fluoro-Jade C (Histo-Chem) in 0.1% acetic acid for 30 min with gentle agitation on ice. Sections were rinsed in water, air-dried and mounted using Permount mounting media. Sections were then imaged using Olympus IX-71 fluorescent microscope as described earlier (Deb et al., 2013). In each slice, the total area in the contralateral side and the non-infarcted area in the lesioned side were measured by an investigator blinded to the experimental conditions using Image J software. The areas on each slide were summed over the numbers of sections evaluated, and the respective volumes were calculated as follows: [(volume of contralateral side – non-infarcted volume of the lesioned side)/volume of contralateral side] × 100% (Swanson et al., 1990).

2.10. Behavioral studies

Male mice treated with vehicle or STEP peptide mimetic (TAT-STEP-Myc peptide) were subjected to neurological assessment and motor function tests (beam balance and rotarod) 24 h after MCAO (30 min) and reperfusion. Habituation to the testing environment and baseline training was performed one week before surgery. An observer blinded to the study groups and treatment conditions evaluated behavioral parameters after surgery. Severity of neurologic deficit (Longa et al., 1989) was assessed on a 5-point scale as follows: 0, no observable deficits; 1, failure to extend left forepaw; 2, circling to the left; 3, falling to left; 4, no spontaneous walking with a depressed level of consciousness; 5, death. For the rotarod test (Allan and Harris, 1989), mice were placed on an accelerating cylinder that rotated from 0 to 50 rpm over a period of 2 min. The time and speed at which the mice fell off the cylinder were measured automatically. For the beam balance test (Crabbe et al., 2003), mice were placed on a metal beam 1.3 cm diameter and 77 cm long, suspended 2 feet above the ground, and were required to traverse the beam. They were scored on a scale of 0–6 as follows: 0, cross the beam without any slips or hesitations; 1, cross the beam with 1 or 2 slips and/or hesitation; 2, cross the beam partially with multiple slips and falls; 3, balances with steady posture (>60 s) with multiple slips and 1 fall; 4, attempts to balance on the beam and falls off (>40 s) with multiple slips and falls but is walking on feet; 5, attempts to balance on the beam but falls off (>20 s), multiple falls and fails to walk on the feet; and 6, falls off: no attempt to balance or hang on the beam (>20 s).

2.11. Statistical analysis

Statistical analysis was conducted with GraphPad Prism 9.0 software (San Diego, CA). All quantitative data are expressed as mean ± standard deviation (SD). Statistical differences between multiple groups were assessed using one-way analysis of variance (ANOVA) followed by Tukey’s post hoc comparisons test. Analysis of simple two group comparison for normally distributed data was done using the Student’s *t*-test. Mean differences between two groups were considered statistically significant when $p < 0.05$.

3. Results

3.1. Early onset and progression of ischemic brain damage in STEP deficient mice

To examine the role of STEP in the temporal progression of ischemic brain injury in the acute phase, WT and STEP KO mice were subjected to MCAO for 30 min followed by reperfusion for 6, 12 and 24 h respectively. Coronal brain sections were then stained with Fluro-Jade C, a fluorescent marker that can recognize the onset of neuronal degeneration following ischemic insult (Butler et al., 2002). The representative photomicrographs (Fig. 1A) and the corresponding bar diagram (Fig. 1B) show an early onset of neurodegeneration in STEP KO mice when compared to WT mice. In the WT mice Fluoro-Jade staining becomes visible only at 12 h of reperfusion that remains limited to the striatum at 24 h. In contrast, significant increase in Fluoro-Jade staining is visible within 6 h of reperfusion in the striatum of STEP KO mice that increases considerably at 12 h of reperfusion, and at 24 h Fluoro-Jade positive cells are present in both the striatum and cortex. Together, these observations suggest that even a mild ischemic insult in the absence of endogenous STEP accelerates the progression of neurodegeneration resulting in exacerbation of ischemic brain damage.

3.2. Increase in neuronal p38 MAPK phosphorylation, COX2 expression and PGE_2 release in STEP deficient mice after ischemic insult

Among the known kinases that are regulated by STEP, p38 MAPK is active in ischemic condition (Barone et al., 2001a, 2001b; Nozaki et al., 2001). To test whether a transient focal ischemia in the absence of STEP has any effect on p38 MAPK phosphorylation, WT and STEP KO mice were subjected to MCAO for varying time periods (10 or 30 min). Immunoblot analysis shows a rapid increase in p38 MAPK phosphorylation in both striatum and cortex of WT (Fig. 2A, C) and STEP KO mice (Fig. 2B, D) within 10 min of the insult. However, in the WT mice p38 MAPK phosphorylation decreases to near basal level by 30 min in both striatum and cortex, while it remains sustained in STEP KO mice. In WT mice, ischemia also leads to de-phosphorylation and subsequent activation of STEP by 30 min as evident from the downward shift in the mobility of the STEP band (Fig. 2A, C), which is consistent with our earlier observation in both cell culture model of excitotoxicity and in animal models of ischemia (Deb et al., 2013; Poddar et al., 2010). As expected, the STEP protein band is not detectable in the tissue lysates from STEP KO mice (Fig. 2B, D). Subsequent studies evaluated the effect of reperfusion after 30 min MCAO, on p38 MAPK phosphorylation in both WT and STEP KO mice. Fig. 2 (E, G) further shows that in the WT mice, p38 MAPK phosphorylation remains at basal levels both at the onset of reperfusion (I/R-0 h) as well as 3 h after the onset of reperfusion (I/R-3 h), and increases only transiently at 6 h after reperfusion (I/R-6 h). This secondary activation of p38 MAPK in WT mice is associated with inactivation of STEP through phosphorylation, as evident from the upward shift in the mobility of the STEP band (Fig. 2E, G). In contrast, p38 MAPK phosphorylation remains continuously elevated in STEP KO mice for at least 6 h after the onset of reperfusion (Fig. 2F, H). A comparative analysis of the magnitude of p38 MAPK phosphorylation at 6 h post-ischemic reperfusion shows a significantly large increase in p38 MAPK phosphorylation in both striatum (~3-fold) and cortex (~4-fold) of STEP KO mice, when compared to WT littermates (Fig. 2I, J). Immunohistochemical staining of coronal

brain sections (ipsilateral cortex) with anti-phospho-p38 MAPK and NeuN antibodies further show that the increase in p38 MAPK phosphorylation in STEP KO mice is localized primarily in neurons (Fig. 2K).

Emerging evidence indicate that depending on the cell type and stimuli, p38 MAPK can enhance transcription and/or stability of COX-2, an enzyme that catalyzes the conversion of arachidonic acid into inflammatory prostaglandins in the post-ischemic brain (Miettinen et al., 1997; Nito et al., 2008; Nogawa et al., 1997; Sasaki et al., 2004; Smith et al., 2000). Therefore, we next investigated the expression of COX-2 in both WT and STEP KO mice, during the ischemic insult and reperfusion. Fig. 4 shows that during the ischemic insult in the WT mice, COX-2 expression remain unchanged as compared to the sham-operated control mice (Fig. 3A, C), while in the STEP KO mice, COX-2 expression increases significantly within 30 min of the insult in the ipsilateral striatum and cortex (Fig. 3B, D). During reperfusion, a transient increase in COX-2 expression is observed 6 h after post-ischemic reperfusion in the WT mice (Fig. 3E, G). In contrast, COX-2 levels in the STEP KO mice increases progressively from the onset of reperfusion through 6 h of post-ischemic reperfusion in both the ipsilateral striatum and cortex (Fig. 3F, H). Comparison of COX-2 protein levels between WT and STEP KO mice at 6 h of post-ischemic reperfusion shows significant increase in COX-2 level in both the striatum (~2-fold) and cortex (~3-fold) of STEP KO mice (Fig. 3I, J). Immunohistochemical staining of the ipsilateral cortex further show that the up regulation of COX-2 protein level in STEP KO mice at 6 h of post-ischemic reperfusion is specifically in neurons (Fig. 3K). PGE_2 immunoassay shows that the elevated COX-2 protein level in the STEP KO mice is associated with significantly higher levels of the inflammatory PGE_2 in both the ipsilateral striatum and cortex of STEP KO mice brain when compared with WT littermates (Fig. 3L, M). The elevated COX-2 expression in neurons and the enhanced PGE_2 production strongly suggests the involvement of neuronal PGE_2 release in increasing post-ischemic inflammatory response in the absence of endogenous STEP.

To determine whether loss of STEP is a key factor in the up regulation of neuronal p38 MAPK-COX2-PGE_2 signaling pathway under ischemic condition, STEP KO mice were subjected to MCAO (30 min) followed by intravenous administration of a single dose of the STEP-peptide mimetic, TAT-STEP-Myc (3 nmol/g; Fig. 4A) at the onset of reperfusion. Restoration of STEP signaling significantly reduced p38 MAPK phosphorylation in both the striatum and cortex of STEP KO mice when treated with the peptide and observed 6 h after reperfusion (Fig. 4B, C). Evaluation of COX-2 protein level (Fig. 4D, E) and PGE_2 level (Fig. 4F, G) at 6 h after reperfusion also show significant reduction in the peptide treated mice.

3.3. Increased microglial activation in STEP deficient mice after ischemic insult

Excessive or persistent release of PGE_2 in the brain has been associated with the activation of microglia that are known to participate in the progression of ischemic pathology (del Zoppo et al., 2007; Kreutzberg, 1996; Mabuchi et al., 2000; Wang et al., 2007). Activated microglia are defined partly by their change in morphology from a ramified state characterized by a small body and multiple thin processes to a more amoeboid shape with

highly branched short processes and increased immunoreactivity for Iba-1 (Ito et al., 2001; Zhang et al., 1997). To investigate whether microglia in STEP KO mice are affected by transient MCAO (30 min) and reperfusion, the morphology of cells immune-reactive for Iba-1 were evaluated in both WT and STEP KO mice brain sections 12 h after reperfusion. Representative microglial phenotype presented in Fig. 5 indicate that change in microglial morphology is not so apparent in either the striatum or cortex of WT mice (Fig. 5A), whereas in the STEP KO mice distinct changes in microglial morphology to the amoeboid form is observed in both the ipsilateral striatum and cortex (Fig. 5B). Quantification of immunofluorescent staining intensity further show a significant increase in immunoreactivity for Iba-1 in the brain of STEP KO mice, when compared with WT littermates (Fig. 5D). Additional studies indicate that administration of the STEP peptide mimetic at the onset of reperfusion blocks change in microglial morphology to the amoeboid state (Fig. 5C) and significantly reduces Iba-1 immunoreactivity (Fig. 5D).

3.4. Increased MMP-9 activity and BBB permeability in STEP deficient mice after ischemic insult

Given that the level and activity of the proteolytic enzyme MMP-9 and subsequent cleavage of tight-junction proteins at the blood–brain barrier (BBB) are regulated by microglia (da Fonseca et al., 2014; Kauppinen and Swanson, 2005; Rivera et al., 2002; Rosenberg et al., 2001; Shigemoto-Mogami et al., 2018), we next investigated MMP-9 activity in the striatum and cortex of both WT and STEP KO mice 18 h after reperfusion. Our findings show a significant increase in MMP-9 activity in the ipsilateral striatum and cortex of STEP KO mice as compared to WT littermates (Fig. 6A, B). Subsequent studies evaluated the endogenous levels of the scaffolding protein ZO-1 and the transmembrane phosphoprotein occludin, two tight junction proteins that are components of the BBB and substrates of MMP-9 (Asahi et al., 2001; Cummins, 2012). While ZO-1 is known to play a role in the regulation of tight junction protein complex through its interaction with occludin and actin cytoskeleton, the monomeric and oligomeric forms of occludin links adjacent endothelial cells to form the paracellular barrier (Cummins, 2012; Furuse et al., 1994; McCaffrey et al., 2007). Our findings show that 24 h after reperfusion in STEP KO mice ZO-1 level is significantly reduced in both the ipsilateral striatum and cortex as compared to the WT littermates (Fig. 6C, D). A significant reduction in the level of the dimeric form of occludin (~125 kDa) is also observed in the ipsilateral striatum and cortex of STEP KO mice, when compared to WT littermates (Fig. 6E, F). Finally, to determine whether BBB permeability changes with the loss of tight junction proteins, we measured the levels of IgG in the ischemic brain from both WT and STEP KO mice 24 h after MCAO and reperfusion (Diamond et al., 2013). Our findings demonstrate that IgG level is significantly elevated in the ipsilateral striatum and cortex of STEP KO mice, when compared to WT littermates (Fig. 6G, H), confirming increased BBB permeability in the absence of STEP.

We next tested whether intravenous administration of the STEP peptide mimetic at the onset of reperfusion has any effect on MMP-9 activity and BBB permeability. For these experiments STEP KO mice were subjected to 30 min MCAO followed by intravenous administration of a single dose of vehicle or STEP-derived peptide (3 nmol/g) at the onset of reperfusion. They were then subjected to reperfusion for the specified time periods. The

extent of MMP-9 activity, analyzed 18 h after post-ischemic reperfusion show a significant decrease in both striatum and cortex of peptide treated mice (Fig. 7A, B). In addition, a significant reduction in extravasation of IgG is observed in the peptide treated mice 24 h after the onset of reperfusion (Fig. 7C, D). Together these findings confirm a role of STEP in regulating a signaling cascade that is involved in the potentiation of post-ischemic inflammatory responses in the brain.

3.5. Post-ischemic functional deficit in STEP deficient mice

To determine whether the significant reduction of inflammatory response in STEP KO mice following treatment with the STEP peptide mimetic could also attenuate neurological and motor deficit, both WT and STEP KO mice were subjected to MCAO (30 min) followed by reperfusion for 24 h. A subset of ischemic STEP KO mice were treated with a single intravenous injection of the STEP peptide mimetic (3 nmol/g) at the onset of reperfusion. At 24 h after reperfusion WT mice shows minimal decline in neurological function as assessed by the modified neurological severity score. In contrast, the STEP KO mice show a severe decline in neurological function (Fig. 8A). Motor function, as assessed by rotarod and beam balance tests also shows a significant decline in STEP KO mice, when compared to the WT littermates (Fig. 8B, C). Intervention with the STEP peptide mimetic shows significantly enhanced neurological and motor function in STEP KO mice, when compared to vehicle-treated STEP KO controls (Fig. 8A–C). Following functional studies, the mice were processed to evaluate the extent of brain damage using Fluoro-Jade staining. The representative photomicrograph shows that deletion of STEP gene leads to exacerbation of ischemic brain injury, while restoration of STEP signaling with intravenous administration of the STEP peptide mimetic reduces ischemic brain damage (Fig. 8D), which is consistent with our earlier finding (Deb et al., 2013). Together these findings confirm a role of STEP in regulating a signaling cascade that is involved in the potentiation of post-ischemic neuroinflammatory response in the brain.

4. Discussion

A key finding of the current study is that in the absence of STEP, focal ischemia evokes an early onset of inflammatory response that begins with rapid and sustained activation of p38MAPK/COX-2/PGE_2 signaling pathway in neurons. The increase in neuronal PGE_2 release in the early stages of ischemia leads to rapid increase in microglial activation and BBB permeability, resulting in exacerbation of ischemic brain injury in STEP KO mice. Consistent with this interpretation, restoration of STEP signaling with intravenous administration of the STEP peptide mimetic attenuates p38MAPK/COX-2/PGE_2 signaling, microglial activity, BBB permeability and ischemic brain damage. These findings strongly suggest that STEP is an upstream regulator of the signaling cascade that triggers post-ischemic neuroinflammation. A schematic representation of this signaling cascade is shown in Fig. 9. The study could lead to a new direction for stroke treatment that could reduce the detrimental impact of inflammation in the early stages of ischemia, without affecting its beneficial factors in the recovery phase.

An important outcome of our study is the distinctly different pattern of p38 MAPK signaling in WT and STEP KO mice following ischemia. In the WT mice, a rapid but transient activation of p38 MAPK in neurons within 10 min of the ischemic insult is followed by a secondary activation of p38 MAPK detected at 6 h post-reperfusion. This biphasic pattern of p38 MAPK activation is consistent with earlier observations in neuron culture models of glutamate excitotoxicity and animal models of ischemic stroke (Deb et al., 2013; Poddar et al., 2010). However, in the STEP KO mice the significant increase in p38 MAPK activation in neurons, observed within 10 min of the insult, remains elevated for at least 6 h after reperfusion. Since STEP inhibits p38 MAPK activation, in the absence of this inhibitory signal the sustained p38 MAPK activation could be an initial trigger for the early onset of inflammatory response in neurons. In conjunction with this finding, we observe a rapid induction of COX-2 expression in neurons within 30 min of the ischemic insult that remains sustained for the duration of p38 MAPK activation. In contrast, only a brief induction of COX-2 is observed in the WT mice 6 h after the onset of reperfusion. Elevated expression and activity of COX-2 is the dominant source of pro-inflammatory PGE_2 synthesis and is a key element in the pathophysiology of several inflammatory disorders (Ricciotti and FitzGerald, 2011). p38 MAPK activation has been shown to increase the stability of COX-2 mRNA in response to a wide range of stimuli and neuronal COX-2 expression has been shown to play a profound role in PGE_2 release, inflammation and neurodegeneration (Bartlett et al., 1999; Dean et al., 1999; Lasa et al., 2000; Park and Kwon, 2011; Ridley et al., 1998; Rockwell et al., 2004; Serrano et al., 2011; Svensson et al., 2003). As such, the significant increase in the PGE_2 level observed in STEP KO mice 6 h after reperfusion could be attributed to the prolonged activation of p38 MAPK-COX-2 pathway in neurons in the absence of STEP.

Increase in COX-2-derived PGE_2 level along with reactive oxygen species generated as a by-product during prostaglandin synthesis are key mediators of microglial activation and have been demonstrated to contribute to post-ischemic neuroinflammation and subsequent brain damage (Candelario-Jalil et al., 2007; Nakamura, 2002; Quan et al., 2013; Smith et al., 2000; Wang et al., 2007; Yenari et al., 2010). Interestingly, in our study the amoeboid morphology reflecting activated state of microglia is observed only in the STEP KO mice as early as 6 h after reperfusion, followed by a large increase in MMP-9 activity observed 18 h after reperfusion. Since microglia is one of the major sources of MMP-9 release following cerebral ischemia (del Zoppo et al., 2012, 2007; Dong et al., 2009; Rosell et al., 2006), these findings further substantiate the role of p38 MAPK-COX-2-PGE_2 signaling pathway in microglial activation in the STEP KO mice. The data also imply that the consequences of COX-2 induction depend largely on the duration and the magnitude of its level. A transient increase in COX-2 level observed in the WT mice fails to exert substantial effect on microglial activity, whereas more prolonged induction of COX-2 level in the STEP KO mice leads to robust microglial activation and inflammation. Further support for this interpretation comes from an earlier study demonstrating that a rapid induction of COX-2 after a mild episode of focal ischemia does not result in tissue inflammation (Planas et al., 2001). In cerebral ischemia, increase in MMP-9 expression and its activity appears to dominate in the acute phase of stroke (Dong et al., 2009; Planas et al., 2001). The presence of high MMP-9 level has been confirmed not only in the infarct tissue but also in the *peri*-infarct areas

suggesting that MMP-9 is involved in process of infarct growth (Dong et al., 2009; Fujimura et al., 1999; Park et al., 2009; Rosell et al., 2006). Such increase in MMP-9 activity in the acute phase of the injury result in cleavage of tight junction proteins leading to disruption of BBB and subsequent infiltration of peripheral immune cells that can contribute to secondary brain damage. (Asahi et al., 2001; Gu et al., 2005; Lohmann et al., 2004; Wang et al., 2009; Yang et al., 2007). In this context, we also observe a significant increase in the cleavage of tight junction proteins ZO-1 and occludin, extravasation of IgG and increase in ischemic brain damage in the STEP KO mice.

The sustained activation of neuronal p38 MAPK-COX-2-PGE_2 signaling cascade and the subsequent increase in microglial activation, MMP-9 activation and BBB dysfunction in the STEP KO mice suggests that STEP constitutes an important control point in the regulation of neuroimmune communication and post-ischemic inflammatory response through modulation of neuronal PGE_2 release. We further evaluated this hypothesis through restoration of STEP signaling with a brain permeable STEP-derived peptide. In earlier studies, we have demonstrated that the phosphorylation of a critical serine residue within the KIM domain of STEP inhibits STEP-p38 MAPK interaction (Poddar et al., 2010). Based on this findings, we generated the STEP-derived peptide where the serine residue in the KIM domain was mutated to allow the peptide to bind irreversibly with p38 MAPK in the absence of the phosphatase domain. Using this peptide, we further showed that when transduced into neurons in culture or injected intravenously in rodents the peptide binds constitutively to p38 MAPK (Poddar et al., 2010, 2019). This unique function of the peptide allowed us to use it as a novel tool to validate the role of STEP in regulating the post-ischemic inflammatory response. Restoring STEP signaling with the administration of the peptide not only attenuated p38 MAPK-COX-2-PGE_2 signaling but also attenuated microglial activation, MMP-9 activity, as well as IgG extravasation. The susceptibility of the STEP KO mice to severe neurological and motor deficits was also attenuated following peptide treatment. These findings substantiate the role of STEP in regulating post- ischemic inflammatory response to minimize stroke damage. The findings also imply that loss of function of endogenous STEP could increase the susceptibility of the brain to ischemic damage due to early onset of the inflammatory response. In this context, we have showed in earlier studies that age-associated increase in oxidative stress leads to inactivation of endogenous STEP (Deb et al., 2011; Rajagopal et al., 2016). Since the majority of strokes (75% − 90%) occur in individuals over the age of 65 and infarct volume as well as mortality rate is higher in aged individuals (Halaweish and Alam, 2015; Yousufuddin and Young, 2019), it would suggest that the STEP-derived peptide could be valuable for the development of novel interventions targeting the post-ischemic inflammatory response, to facilitate better recovery and reduce mortality in the aged population.

The current study focuses on the role of STEP in regulating p38 MAPK-mediated post-ischemic inflammatory response using the STEP deficient mice. However, additional STEP substrates that include ERK1/2 and the non-receptor tyrosine kinases Pyk2 and Fyn may also be involved in inducing post-ischemic inflammatory responses. Indeed, several studies have established the role of Pyk2 and Fyn in ischemic brain damage, although the involvement of ERK1/2 in cerebral ischemia still remains controversial. (Alessandrini et al., 1999; Jover-Mengual et al., 2007; Kong et al., 2019; Paul et al., 2001; Tian et al., 2000; Xu

et al., 2012). Therefore, to further our understanding of additional inflammatory pathways that may be regulated by STEP, future studies will focus on identification of other STEP substrates that are upregulated in the STEP deficient mice after an ischemic insult, evaluation of their role in inducing inflammatory response and the contribution of the STEP-peptide mimetic in regulating them.

In conclusion, the findings strongly imply that predisposition to comorbidities, which compromise STEP function could exacerbate ischemic brain injury by enhancing inflammatory response. To the best of our knowledge this study demonstrates for the first time the role of a tyrosine phosphatase in regulating inflammatory pathways in the brain and suggests that the STEP enzyme may play a far more important role in brain function than just regulating ischemia-induced brain injury. The study also highlights the therapeutic potential of the STEP-derived peptide in a wide spectrum of neurological disorders where excitotoxicity contributes to brain damage through activation of neuroinflammatory pathways.

Acknowledgements

This work was supported by the National Institute of Health grant numbers RO1 NS059962 (Paul, S) and RO1 NS083914 (Poddar, R) and RO1 NS103094 and RO1 NS109816 (Candelario-Jalil, E).

References

Alessandrini A, Namura S, Moskowitz MA, Bonventre JV, 1999. MEK1 protein kinase inhibition protects against damage resulting from focal cerebral ischemia. PNAS 96 (22), 12866–12869. [PubMed: 10536014]

Allan AM, Harris RA, 1989. A new alcohol antagonist: phaclofen. Life Sci. 45 (19), 1771–1779. [PubMed: 2556616]

Arundine M, Tymianski M, 2004. Molecular mechanisms of glutamate-dependent neurodegeneration in ischemia and traumatic brain injury. Cell Mol. Life Sci 61 (6), 657–668. [PubMed: 15052409]

Asahi M, Wang X, Mori T, Sumii T, Jung J-C, Moskowitz MA, Fini ME, Lo EH, 2001. Effects of matrix metalloproteinase-9 gene knock-out on the proteolysis of blood-brain barrier and white matter components after cerebral ischemia. J. Neurosci 21 (19), 7724–7732. [PubMed: 11567062]

Barone FC, Irving EA, Ray AM, Lee JC, Kassis S, Kumar S, Badger AM, Legos JJ, Erhardt JA, Ohlstein EH, Hunter AJ, Harrison DC, Philpott K, Smith BR, Adams JL, Parsons AA, 2001a. Inhibition of p38 mitogen-activated protein kinase provides neuroprotection in cerebral focal ischemia. Med. Res. Rev 21 (2), 129–145. [PubMed: 11223862]

Barone FC, Irving EA, Ray AM, Lee JC, Kassis S, Kumar S, Badger AM, White RF, McVey MJ, Legos JJ, et al., 2001b. SB 239063, a second-generation p38 mitogen-activated protein kinase inhibitor, reduces brain injury and neurological deficits in cerebral focal ischemia. J. Pharmacol. Experimental Therapeutics 296, 312–321.

Bartlett SR, Sawdy R, Mann GE, 1999. Induction of cyclooxygenase-2 expression in human myometrial smooth muscle cells by interleukin-1beta: involvement of p38 mitogen-activated protein kinase. J. Physiol 520 (Pt 2), 399–406. [PubMed: 10523409]

Boulanger LM, Lombroso PJ, Raghunathan A, During MJ, Wahle P, Naegele JR, 1995. Cellular and molecular characterization of a brain-enriched protein tyrosine phosphatase. J. Neurosci 15 (2), 1532–1544. [PubMed: 7869116]

Butler TL, Kassed CA, Sanberg PR, Willing AE, Pennypacker KR, 2002. Neurodegeneration in the rat hippocampus and striatum after middle cerebral artery occlusion. Brain Res. 929 (2), 252–260. [PubMed: 11864631]

Candelario-Jalil E, Gonzalez-Falcon A, Garcia-Cabrera M, Leon OS, Fiebich BL, 2007. Post-ischaemic treatment with the cyclooxygenase-2 inhibitor nimesulide reduces blood-brain barrier disruption and leukocyte infiltration following transient focal cerebral ischaemia in rats. J. Neurochem 100, 1108–1120. [PubMed: 17176264]

Crabbe JC, Metten P, Yu C-H, Schlumbohm JP, Cameron AJ, Wahlsten D, 2003. Genotypic differences in ethanol sensitivity in two tests of motor incoordination. J. Appl. Physiol 95 (4), 1338–1351. [PubMed: 12704090]

Cummins PM, 2012. Occludin: one protein, many forms. Mol. Cell Biol 32 (2), 242–250. [PubMed: 22083955]

da Fonseca AC, Matias D, Garcia C, Amaral R, Geraldo LH, Freitas C, Lima FR, 2014. The impact of microglial activation on blood-brain barrier in brain diseases. Front. Cell Neurosci 8, 362. [PubMed: 25404894]

Dean JLE, Brook M, Clark AR, Saklatvala J, 1999. p38 mitogen-activated protein kinase regulates cyclooxygenase-2 mRNA stability and transcription in lipopolysaccharide-treated human monocytes. J. Biol. Chem 274 (1), 264–269. [PubMed: 9867839]

Deb I, Manhas N, Poddar R, Rajagopal S, Allan AM, Lombroso PJ, Rosenberg GA, Candelario-Jalil E, Paul S, 2013. Neuroprotective role of a brain-enriched tyrosine phosphatase, STEP, in focal cerebral ischemia. J. Neurosci 33 (45), 17814–17826. [PubMed: 24198371]

Deb I, Poddar R, Paul S, 2011. Oxidative stress-induced oligomerization inhibits the activity of the non-receptor tyrosine phosphatase STEP61. J. Neurochem 116, 1097–1111. [PubMed: 21198639]

del Zoppo GJ, Frankowski H, Gu Y-H, Osada T, Kanazawa M, Milner R, Wang X, Hosomi N, Mabuchi T, Koziol JA, 2012. Microglial cell activation is a source of metalloproteinase generation during hemorrhagic transformation. J. Cereb Blood Flow Metab 32 (5), 919–932. [PubMed: 22354151]

del Zoppo GJ, Milner R, Mabuchi T, Hung S, Wang X, Berg GI, Koziol JA, 2007. Microglial activation and matrix protease generation during focal cerebral ischemia. Stroke 38 (2), 646–651. [PubMed: 17261708]

Diamond B, Honig G, Mader S, Brimberg L, Volpe BT, 2013. Brain-reactive antibodies and disease. Annu. Rev. Immunol 31 (1), 345–385. [PubMed: 23516983]

Dong X, Song YN, Liu WG, Guo XL, 2009. Mmp-9, a potential target for cerebral ischemic treatment. Curr. Neuropharmacol 7, 269–275. [PubMed: 20514206]

Fujimura M, Gasche Y, Morita-Fujimura Y, Massengale J, Kawase M, Chan PH, 1999. Early appearance of activated matrix metalloproteinase-9 and blood-brain barrier disruption in mice after focal cerebral ischemia and reperfusion. Brain Res. 842 (1), 92–100. [PubMed: 10526099]

Furuse M, Itoh M, Hirase T, Nagafuchi A, Yonemura S, Tsukita S, Tsukita S, 1994. Direct association of occludin with ZO-1 and its possible involvement in the localization of occludin at tight junctions. J. Cell Biol 127, 1617–1626. [PubMed: 7798316]

Gu Z, Cui J, Brown S, Fridman R, Mobashery S, Strongin AY, Lipton SA, 2005. A highly specific inhibitor of matrix metalloproteinase-9 rescues laminin from proteolysis and neurons from apoptosis in transient focal cerebral ischemia. J. Neurosci 25, 6401–6408. [PubMed: 16000631]

Halaweish I, Alam HB, 2015. Changing demographics of the American population. Surg. Clin. North Am 95 (1), 1–10. [PubMed: 25459538]

Hawkins KE, DeMars KM, Yang C, Rosenberg GA, Candelario-Jalil E, 2013. Fluorometric immunocapture assay for the specific measurement of matrix metalloproteinase-9 activity in biological samples: application to brain and plasma from rats with ischemic stroke. Mol. Brain 6 (1), 14. 10.1186/1756-6606-6-14. [PubMed: 23522154]

Hoque A, Hossain MI, Ameen SS, Ang C-S, Williamson N, Ng DCH, Chueh AC, Roulston C, Cheng H-C, 2016. A beacon of hope in stroke therapy-Blockade of pathologically activated cellular events in excitotoxic neuronal death as potential neuroprotective strategies. Pharmacol. Ther 160, 159–179. [PubMed: 26899498]

Howard G, Toole JF, Frye-Pierson J, Hinshelwood LC, 1987. Factors influencing the survival of 451 transient ischemic attack patients. Stroke; J. Cerebral Circulation 18 (3), 552–557.

Hoyte L, Barber PA, Buchan AM, Hill MD, 2004. The rise and fall of NMDA antagonists for ischemic stroke. Curr. Mol. Med 4, 131–136. [PubMed: 15032709]

Ikonomidou C, Turski L, 2002. Why did NMDA receptor antagonists fail clinical trials for stroke and traumatic brain injury? Lancet Neurol. 1 (6), 383–386. [PubMed: 12849400]

Ito D, Tanaka K, Suzuki S, Dembo T, Fukuuchi Y, 2001. Enhanced expression of Iba1, ionized calcium-binding adapter molecule 1, after transient focal cerebral ischemia in rat brain. Stroke 32 (5), 1208–1215. [PubMed: 11340235]

Jover-Mengual T, Zukin RS, Etgen AM, 2007. MAPK signaling is critical to estradiol protection of CA1 neurons in global ischemia. Endocrinology 148 (3), 1131–1143. [PubMed: 17138646]

Kauppinen TM, Swanson RA, 2005. Poly(ADP-ribose) polymerase-1 promotes microglial activation, proliferation, and matrix metalloproteinase-9-mediated neuron death. J. Immunol 174 (4), 2288–2296. [PubMed: 15699164]

Kong T, Liu M, Ji B, Bai B, Cheng B, Wang C, 2019. Role of the Extracellular Signal-Regulated Kinase 1/2 Signaling Pathway in Ischemia-Reperfusion Injury. Front. Physiol 10, 1038. [PubMed: 31474876]

Kreutzberg GW, 1996. Microglia: a sensor for pathological events in the CNS. Trends Neurosci. 19 (8), 312–318. [PubMed: 8843599]

Lasa M, Mahtani KR, Finch A, Brewer G, Saklatvala J, Clark AR, 2000. Regulation of cyclooxygenase 2 mRNA stability by the mitogen-activated protein kinase p38 signaling cascade. Mol. Cell Biol 20 (12), 4265–4274. [PubMed: 10825190]

Lau A, Tymianski M, 2010. Glutamate receptors, neurotoxicity and neurodegeneration. Pflugers Arch. 460 (2), 525–542. [PubMed: 20229265]

Liu Y, Wong TP, Aarts M, Rooyakkers A, Liu L, Lai TW, Wu DC, Lu J, Tymianski M, Craig AM, Wang YT, 2007. NMDA receptor subunits have differential roles in mediating excitotoxic neuronal death both in vitro and in vivo. J. Neurosci 27 (11), 2846–2857. [PubMed: 17360906]

Lohmann C, Krischke M, Wegener J, Galla H-J, 2004. Tyrosine phosphatase inhibition induces loss of blood-brain barrier integrity by matrix metalloproteinase- dependent and -independent pathways. Brain Res. 995 (2), 184–196. [PubMed: 14672808]

Lombroso PJ, Naegele JR, Sharma E, Lerner M, 1993. A protein tyrosine phosphatase expressed within dopaminoceptive neurons of the basal ganglia and related structures. J. Neurosci 13 (7), 3064–3074. [PubMed: 8331384]

Longa EZ, Weinstein PR, Carlson S, Cummins R, 1989. Reversible middle cerebral artery occlusion without craniectomy in rats. Stroke 20 (1), 84–91. [PubMed: 2643202]

Mabuchi T, Kitagawa K, Ohtsuki T, Kuwabara K, Yagita Y, Yanagihara T, Hori M, Matsumoto M, 2000. Contribution of microglia/macrophages to expansion of infarction and response of oligodendrocytes after focal cerebral ischemia in rats. Stroke 31 (7), 1735–1743. [PubMed: 10884481]

McCaffrey G, Staatz WD, Quigley CA, Nametz N, Seelbach MJ, Campos CR, Brooks TA, Egleton RD, Davis TP, 2007. Tight junctions contain oligomeric protein asSDbly critical for maintaining blood-brain barrier integrity in vivo. J. Neurochem 103, 2540–2555. [PubMed: 17931362]

Miettinen S, Fusco FR, Yrjanheikki J, Keinanen R, Hirvonen T, Roivainen R, Narhi M, Hokfelt T, Koistinaho J, 1997. Spreading depression and focal brain ischemia induce cyclooxygenase-2 in cortical neurons through N-methyl-D-aspartic acid-receptors and phospholipase A2. PNAS 94 (12), 6500–6505. [PubMed: 9177247]

Mukherjee S, Poddar R, Deb I, Paul S, 2011. Dephosphorylation of specific sites in the kinase-specificity sequence domain leads to ubiquitin-mediated degradation of the tyrosine phosphatase STEP. Biochem. J 440, 115–125. [PubMed: 21777200]

Nakamura Y, 2002. Regulating factors for microglial activation. Biol. Pharm Bull 25 (8), 945–953. [PubMed: 12186424]

Nakayama H, Jørgensen HS, Raaschou HO, Olsen TS, 1994. The influence of age on stroke outcome. The Copenhagen Stroke Study. Stroke; J. Cerebral Circulation 25 (4), 808–813.

Nito C, Kamada H, Endo H, Niizuma K, Myer DJ, Chan PH, 2008. Role of the p38 mitogen-activated protein kinase/cytosolic phospholipase A2 signaling pathway in blood-brain barrier disruption after focal cerebral ischemia and reperfusion. J. Cereb. Blood Flow Metab 28 (10), 1686–1696. [PubMed: 18545259]

Nogawa S, Zhang F, Ross ME, Iadecola C, 1997. Cyclo-oxygenase-2 gene expression in neurons contributes to ischemic brain damage. J. Neurosci 17 (8), 2746–2755. [PubMed: 9092596]

Nozaki K, Nishimura M, Hashimoto N, 2001. Mitogen-activated protein kinases and cerebral ischemia. Mol. Neurobiol 23 (1), 01–20.

Park EJ, Kwon TK, 2011. Rottlerin enhances IL-1beta-induced COX-2 expression through sustained p38 MAPK activation in MDA-MB-231 human breast cancer cells. Exp. Mol. Med 43, 669–675. [PubMed: 21971413]

Park K-P, Rosell A, Foerch C, Xing C, Kim WJ, Lee S, Opdenakker G, Furie KL, Lo EH, 2009. Plasma and brain matrix metalloproteinase-9 after acute focal cerebral ischemia in rats. Stroke 40 (8), 2836–2842. [PubMed: 19556529]

Patel AR, Ritzel R, McCullough LD, Liu F, 2013. Microglia and ischemic stroke: a double-edged sword. Int. J. Physiol. Pathophysiol. Pharmacol 5, 73–90. [PubMed: 23750306]

Paul R, Zhang ZG, Eliceiri BP, Jiang Q, Boccia AD, Zhang RL, Chopp M, Cheresh DA, 2001. Src deficiency or blockade of Src activity in mice provides cerebral protection following stroke. Nat. Med 7 (2), 222–227. [PubMed: 11175854]

Paul S, Connor J, 2010. NR2B-NMDA receptor mediated increases in intracellular Ca2 + concentration regulate the tyrosine phosphatase, STEP, and ERK MAP kinase signaling. J. Neurochem. In Press

Paul S, Nairn AC, Wang P, Lombroso PJ, 2003. NMDA-mediated activation of the tyrosine phosphatase STEP regulates the duration of ERK signaling. Nat. Neurosci 6 (1), 34–42. [PubMed: 12483215]

Paul S, Snyder GL, Yokakura H, Picciotto MR, Nairn AC, Lombroso PJ, 2000. The Dopamine/D1 receptor mediates the phosphorylation and inactivation of the protein tyrosine phosphatase STEP via a PKA-dependent pathway. J. Neurosci 20 (15), 5630–5638. [PubMed: 10908600]

Planas AM, Solé S, Justicia C, 2001. Expression and activation of matrix metalloproteinase-2 and −9 in rat brain after transient focal cerebral ischemia. Neurobiol. Dis 8 (5), 834–846. [PubMed: 11592852]

Poddar R, Deb I, Mukherjee S, Paul S, 2010. NR2B-NMDA receptor mediated modulation of the tyrosine phosphatase STEP regulates glutamate induced neuronal cell death. J. Neurochem 115, 1350–1362. [PubMed: 21029094]

Poddar R, Rajagopal S, Shuttleworth CW, Paul S, 2016. Zn2+-dependent Activation of the Trk Signaling Pathway Induces Phosphorylation of the Brain-enriched Tyrosine Phosphatase STEP: MOLECULAR BASIS FOR ZN2+-INDUCED ERK MAPK ACTIVATION. J. Biol. Chem 291 (2), 813–825. [PubMed: 26574547]

Poddar R, Rajagopal S, Winter L, Allan AM, Paul S, 2019. A peptide mimetic of tyrosine phosphatase STEP as a potential therapeutic agent for treatment of cerebral ischemic stroke. J. Cereb. Blood Flow Metab 39 (6), 1069–1084. [PubMed: 29215306]

Quan Y.i., Jiang J, Dingledine R, 2013. EP2 receptor signaling pathways regulate classical activation of microglia. J. Biol. Chem 288 (13), 9293–9302. [PubMed: 23404506]

Rajagopal S, Deb I, Poddar R, Paul S, 2016. Aging is associated with dimerization and inactivation of the brain-enriched tyrosine phosphatase STEP. Neurobiol. Aging 41, 25–38. [PubMed: 27103516]

Ricciotti E, FitzGerald GA, 2011. Prostaglandins and inflammation. Arterioscler. Thromb. Vasc Biol 31 (5), 986–1000. [PubMed: 21508345]

Ridley SH, Dean JL, Sarsfield SJ, Brook M, Clark AR, Saklatvala J, 1998. A p38 MAP kinase inhibitor regulates stability of interleukin-1-induced cyclooxygenase-2 mRNA. FEBS Lett. 439, 75–80. [PubMed: 9849881]

Rivera S, Ogier C, Jourquin J, Timsit S, Szklarczyk AW, Miller K, Gearing AJH, Kaczmarek L, Khrestchatisky M, 2002. Gelatinase B and TIMP-1 are regulated in a cell- and time-dependent manner in association with neuronal death and glial reactivity after global forebrain ischemia. Eur. J. Neurosci 15 (1), 19–32. [PubMed: 11860503]

Rockwell P, Martinez J, Papa L, Gomes E, 2004. Redox regulates COX-2 upregulation and cell death in the neuronal response to cadmium. Cell. Signal 16, 343–353. [PubMed: 14687664]

Rosell A, Ortega-Aznar A, Alvarez-Sabín José, Fernández-Cadenas I, Ribó M, Molina CA, Lo EH, Montaner J, 2006. Increased brain expression of matrix metalloproteinase-9 after ischemic and hemorrhagic human stroke. Stroke; J. Cerebral Circulation 37 (6), 1399–1406.

Rosenberg GA, Cunningham LA, Wallace J, Alexander S, Estrada EY, Grossetete M, Razhagi A, Miller K, Gearing A, 2001. Immunohistochemistry of matrix metalloproteinases in reperfusion injury to rat brain: activation of MMP-9 linked to stromelysin-1 and microglia in cell cultures. Brain Res. 893 (1–2), 104–112. [PubMed: 11222998]

Sasaki T, Kitagawa K, Yamagata K, Takemiya T, Tanaka S, Omura-Matsuoka E, Sugiura S, Matsumoto M, Hori M, 2004. Amelioration of hippocampal neuronal damage after transient forebrain ischemia in cyclooxygenase-2-deficient mice. J. Cereb. Blood Flow Metab 24 (1), 107–113. [PubMed: 14688622]

Serrano GE, Lelutiu N, Rojas A, Cochi S, Shaw R, Makinson CD, Wang D, FitzGerald GA, Dingledine R, 2011. Ablation of cyclooxygenase-2 in forebrain neurons is neuroprotective and dampens brain inflammation after status epilepticus. J. Neurosci 31 (42), 14850–14860. [PubMed: 22016518]

Shigemoto-Mogami Y, Hoshikawa K, Sato K, 2018. Activated Microglia Disrupt the Blood-Brain Barrier and Induce Chemokines and Cytokines in a Rat in vitro Model. Front. Cell Neurosci 12, 494. [PubMed: 30618641]

Smith WL, DeWitt DL, Garavito RM, 2000. Cyclooxygenases: structural, cellular, and molecular biology. Annu. Rev. Biochem 69 (1), 145–182. [PubMed: 10966456]

Svensson CI, Hua X-Y, Protter AA, Powell HC, Yaksh TL, 2003. Spinal p38 MAP kinase is necessary for NMDA-induced spinal PGE(2) release and thermal hyperalgesia. NeuroReport 14 (8), 1153–1157. [PubMed: 12821799]

Swanson RA, Morton MT, Tsao-Wu G, Savalos RA, Davidson C, Sharp FR, 1990. A SDiautomated method for measuring brain infarct volume. J. Cereb. Blood Flow Metab 10, 290–293. [PubMed: 1689322]

Tian D, Litvak V, Lev S, 2000. Cerebral ischemia and seizures induce tyrosine phosphorylation of PYK2 in neurons and microglial cells. J. Neurosci 20 (17), 6478–6487. [PubMed: 10964954]

Venkitaramani DV, Paul S, Zhang Y, Kurup P, Ding L.i., Tressler L, Allen M, Sacca R, Picciotto MR, Lombroso PJ, 2009. Knockout of striatal enriched protein tyrosine phosphatase in mice results in increased ERK1/2 phosphorylation. Synapse (New York. NY 63 (1), 69–81.

Wang G, Guo Q, Hossain M, Fazio V, Zeynalov E, Janigro D, Mayberg MR, Namura S, 2009. Bone marrow-derived cells are the major source of MMP-9 contributing to blood-brain barrier dysfunction and infarct formation after ischemic stroke in mice. Brain Res. 1294, 183–192. [PubMed: 19646426]

Wang Q, Tang X, Yenari M, 2007. The inflammatory response in stroke. J. Neuroimmunol 184 (1–2), 53–68. [PubMed: 17188755]

Xu J, Kurup P, Bartos JA, Patriarchi T, Hell JW, Lombroso PJ, 2012. Striatal- enriched protein-tyrosine phosphatase (STEP) regulates Pyk2 kinase activity. J. Biol. Chem 287 (25), 20942–20956. [PubMed: 22544749]

Yang Y, Estrada EY, Thompson JF, Liu W, Rosenberg GA, 2007. Matrix metalloproteinase-mediated disruption of tight junction proteins in cerebral vessels is reversed by synthetic matrix metalloproteinase inhibitor in focal ischemia in rat. J. Cereb. Blood Flow Metab 27 (4), 697–709. [PubMed: 16850029]

Yang Y, Salayandia VM, Thompson JF, Yang LY, Estrada EY, Yang Y.i., 2015. Attenuation of acute stroke injury in rat brain by minocycline promotes blood-brain barrier remodeling and alternative microglia/macrophage activation during recovery. J. Neuroinflammation 12 (1), 26. 10.1186/s12974-015-0245-4. [PubMed: 25889169]

Yenari MA, Kauppinen TM, Swanson RA, 2010. Microglial activation in stroke: therapeutic targets. Neurotherapeutics : J. Am. Soc. Experim. NeuroTherapeutics 7 (4), 378–391.

Yousufuddin M, and Young N, 2019. Aging and ischemic stroke. Aging (Albany NY) 11, 2542–2544. [PubMed: 31043575]

Zhang Z, Chopp M, Powers C, 1997. Temporal profile of microglial response following transient (2 h) middle cerebral artery occlusion. Brain Res. 744 (2), 189–198. [PubMed: 9027378]

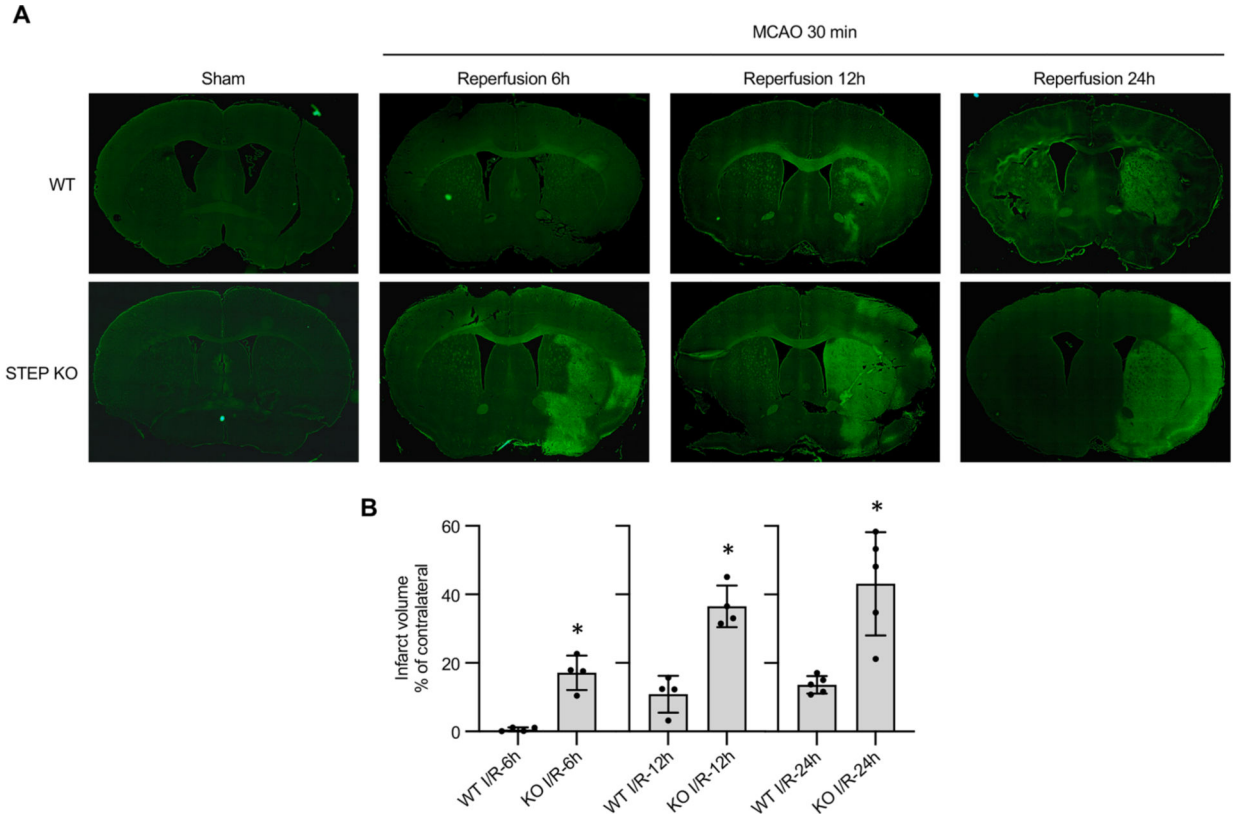

Fig. 1. Cerebral ischemic insult accelerates the progression of brain injury in STEP KO mice.

WT and STEP KO mice were subjected to MCAO for 30 min followed by reperfusion for the specified time periods (6, 12 and 24 h). Coronal brain sections from WT and STEP KO mice were stained with Fluoro-Jade C, a marker for cellular degeneration. (a) Representative photomicrographs of coronal brain sections through the striatum demonstrating the progression of ischemic brain damage in WT and STEP KO mice. (b) Corresponding bar diagram represents quantitative analysis of total infarct volume in WT and STEP KO mice as mean ± SD (n = 3–5 mice / group). *$p < 0.01$ from corresponding WT mice subjected to ischemia/reperfusion (I/R) for the specified time period.

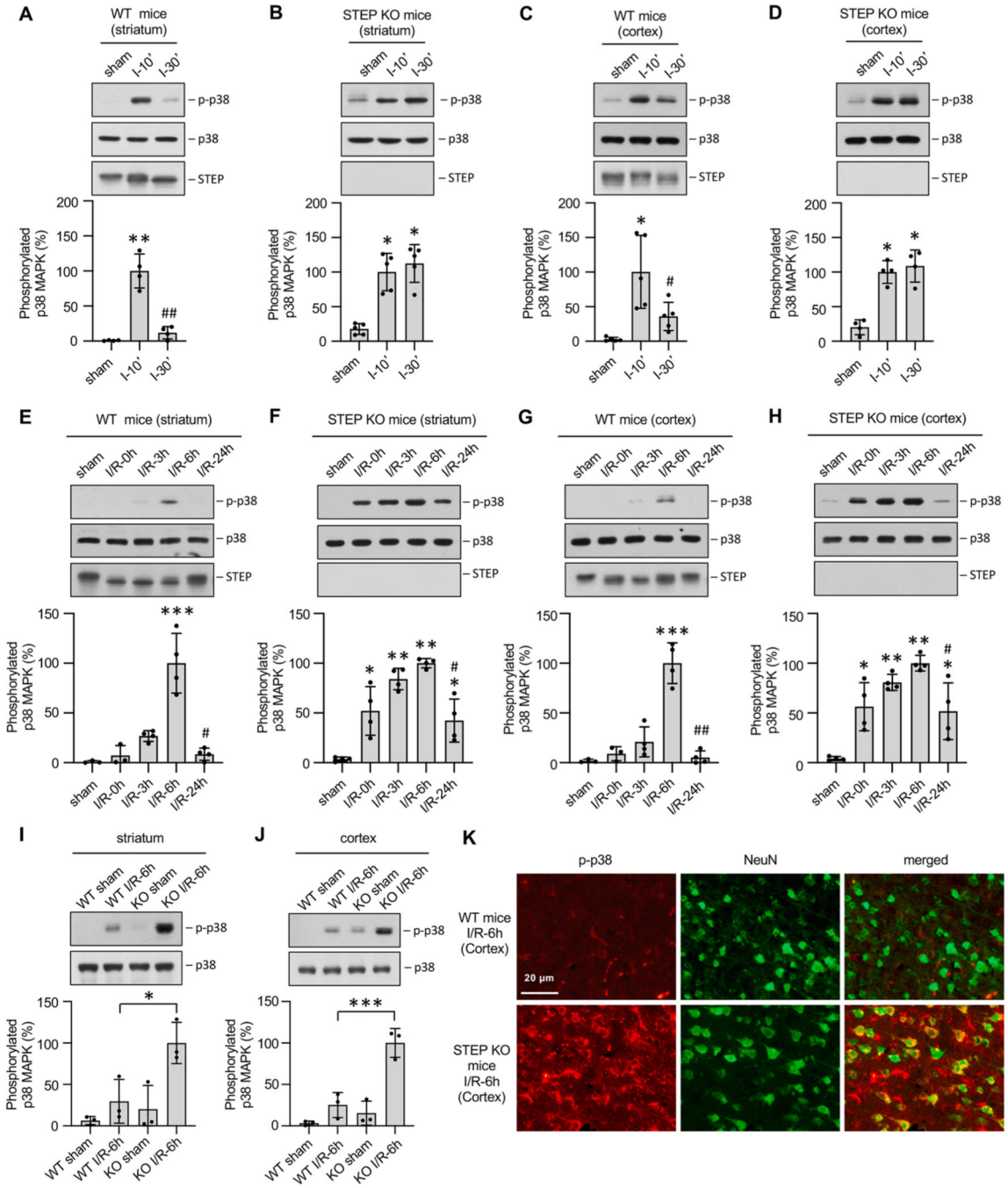

Fig. 2. Sustained increase in p38 MAPK phosphorylation in STEP KO mice during ischemia and reperfusion.

(A, C) WT and (B, D) STEP KO mice were subjected to sham surgery or MCAO (I) for the specified time periods (10 and 30 min). (E, G) WT and (F, H) STEP KO mice were subjected to sham surgery or MCAO (I) for 30 min followed by reperfusion (R) for the specified time periods (0, 3, 6 and 24 h). Tissue extracts with equal amount of protein from the ipsilateral (A, B, E, F) striatum and (C, D, G, H) cortex was analyzed with anti-phospho-p38 MAPK (upper panels). Equal protein loading in each sample was confirmed by re-probing the blots with anti-p38 MAPK antibody (middle panels). STEP was analyzed by

immunoblotting with anti-STEP (lower panels) antibody. (I, J) The increase in p38 MAPK phosphorylation in the (I) striatum and (J) cortex of WT and STEP KO mice at 6 h post-MCAO reperfusion time point was compared by immunoblot analysis using anti-phospho-p38 MAPK antibody (upper panels) and anti-p38 MAPK antibody (lower panels). (A-D) Bar diagrams represents mean ± SD (n = 4–5 mice / group). *$p < 0.05$ and **$p < 0.001$ from sham; $^{\#}p < 0.05$ and $^{\#\#}p < 0.001$ from MCAO 10 min (I-10′). (E-J) Bar diagrams represent mean ± SD (n = 3–4 mice / group). (E-H) *$p < 0.01$, **$p < 0.001$ and ***$p < 0.0001$ from sham; $^{\#}p < 0.01$ and $^{\#\#}p < 0.0001$ from 6 h post-ischemic reperfusion (I/R-6 h). (I, J) *$p < 0.01$ and ***$p < 0.0001$ from WT I/R-6 h. (K) WT and STEP KO mice were subjected to 30 min MCAO followed by reperfusion for 6 h and then processed for immunohistochemical analysis with anti-phospho-p38-MAPK and NeuN antibodies. Representative photomicrographs demonstrating phospho-p38 MAPK and NeuN positive cells in the ipsilateral cortex.

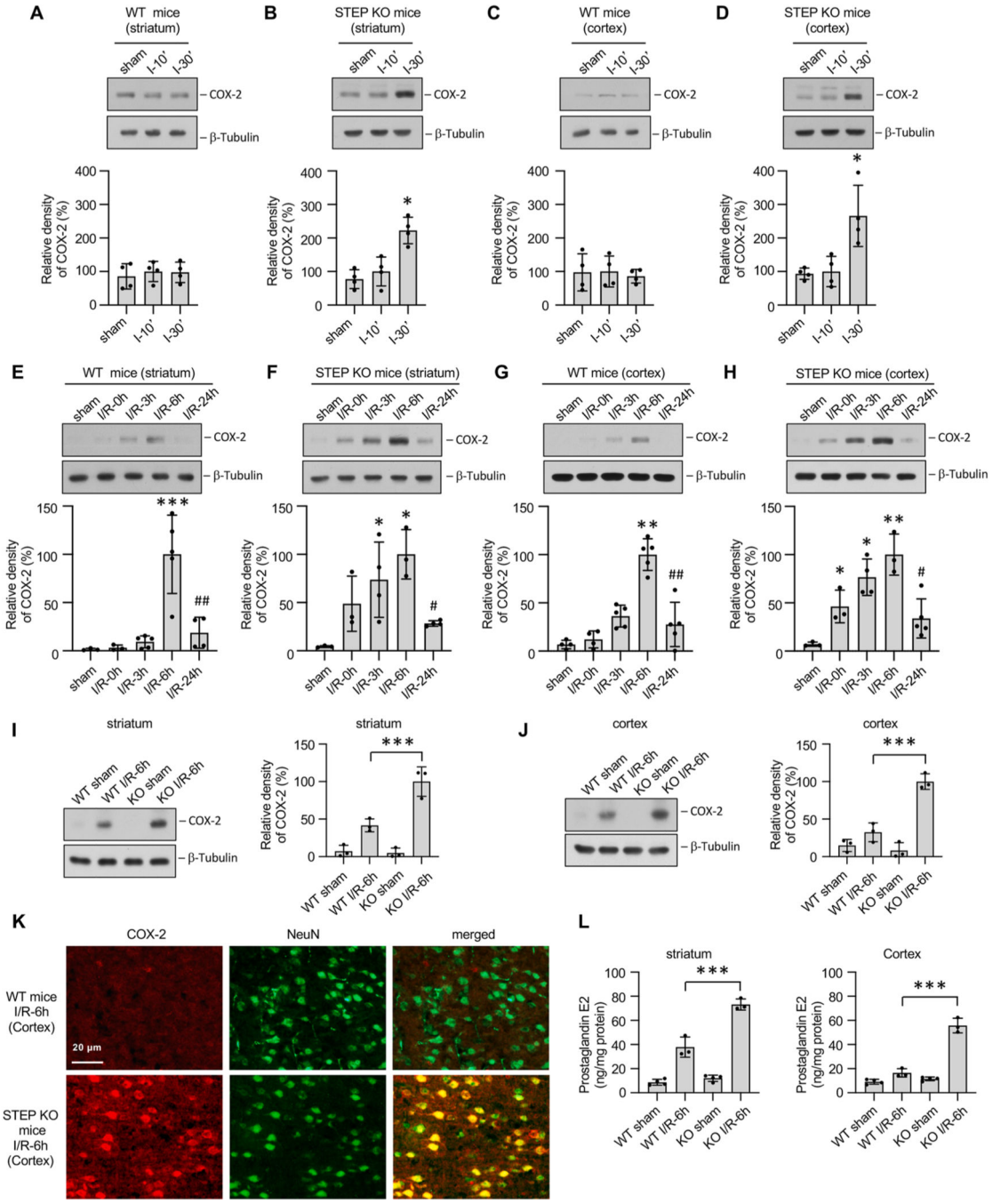

Fig. 3. Increase in COX-2 protein and prostaglandin E_2 levels in STEP KO mice during ischemia and reperfusion.

(A, C) WT and (B, D) STEP KO mice were subjected to sham surgery or MCAO (I) for the specified time periods (10 and 30 min). (E, G) WT and (F, H) STEP KO mice were subjected to sham surgery or MCAO (I) for 30 min followed by reperfusion (R) for the specified time periods (0, 3, 6 and 24 h). COX-2 protein levels in tissue lysates from the ipsilateral (A, B, E, F) striatum and (C, D, G, H) cortex was analyzed with anti-COX-2 antibody (upper panels). Equal protein loading in each sample was confirmed by re-probing the blots with anti-β-tubulin antibody (lower panels). (I, J) The increase in COX-2 level in

the striatum and cortex of WT and STEP KO mice at 6 h post-MCAO reperfusion time point was compared by immunoblot analysis, using anti-COX-2 antibody (upper panels) and anti-β-tubulin antibody (lower panels). (A-D) Bar diagrams represents mean ± SD (n = 4 mice / group). *$p < 0.01$ from sham. (E-J) Bar diagrams represent mean ± SD (n = 3–5 mice/ group). (E-H) *$p < 0.05$, **$p < 0.001$ and ***$p < 0.0001$ from sham; $^{\#}p < 0.05$ and $^{\#\#}p < 0.001$ from 6 h post-ischemic reperfusion (I/R-6 h). (I, J) ***$p < 0.0001$ from WT I/R-6 h. (K) WT and STEP KO mice were subjected to 30 min MCAO followed by reperfusion for 6 h and then processed for immunohistochemistry with anti-COX-2 and NeuN antibodies. Representative photomicrographs demonstrating COX-2 and NeuN positive cells in the ipsilateral cortex. (L) WT and (M) STEP KO mice were subjected to sham surgery or 30 min MCAO followed by reperfusion for 6 h. PGE_2 level was measured by enzyme immunoassay in the supernatants obtained from ipsilateral striatum and cortex of both WT and STEP KO mice. Data are expressed as nanograms (ng) of PGE_2 level per milligram (mg) of cellular protein. Bar diagram represent mean ± SD (n = 3–4 mice / group) and ***$p < 0.0001$ between WT I/R 6 h and KO I/R 6 h.

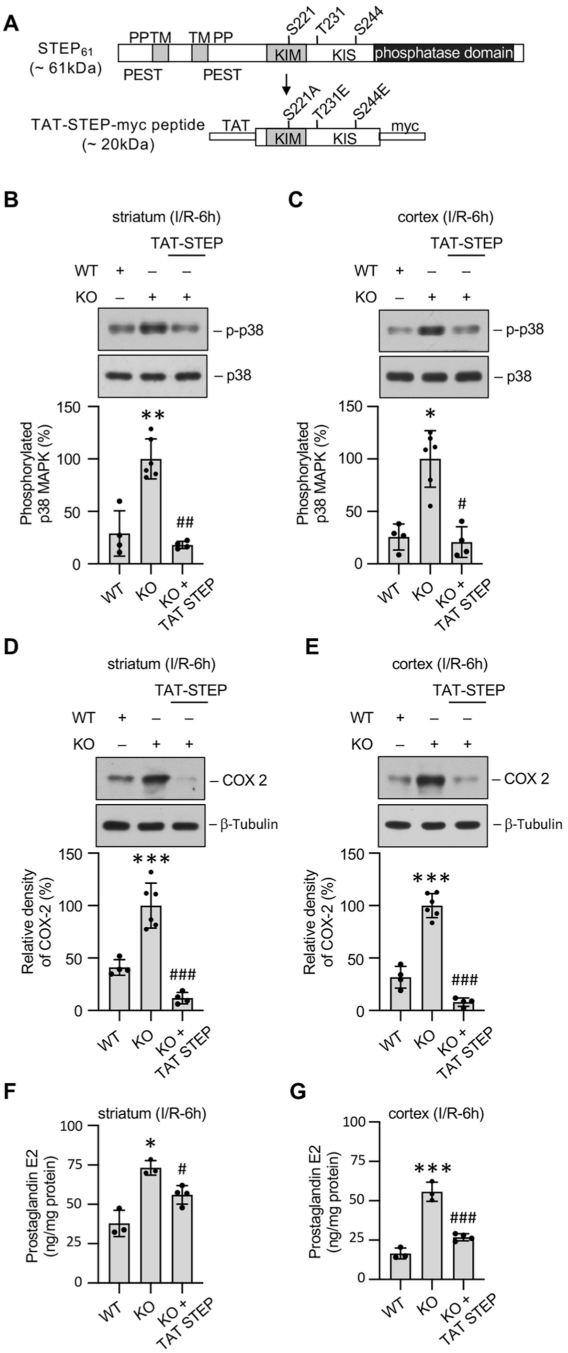

Fig. 4. STEP mimetic attenuates post-ischemic increase in p38 MAPK phosphorylation, COX-2 expression and PGE_2 release in STEP KO mice.

(A) Schematic representation of TAT-STEP-Myc peptide generated from $STEP_{61}$. Diagram of $STEP_{61}$ indicating the positions of the phosphatase domain, putative proteolytic sites (PEST), transmembrane domain (TM), polyproline rich regions (PP), kinase interacting motif (KIM), kinase specificity sequence (KIS) and known phosphorylation sites. The STEP mimetic (TAT-STEP-Myc peptide) derived from $STEP_{61}$ was rendered cell-permeable by fusion to the 11 amino acid protein transduction domain (TAT) of the human immunodeficiency virus-type I at the N-terminus and has a Myc-tag at the C-terminus. The

serine residue in the kinase interacting motif (KIM) was mutated to alanine to allow the peptide to bind constitutively with its substrates. The threonine and serine residues in the kinase specificity sequence (KIS) were mutated to glutamic acid to render the peptide resistant to degradation. (B-G) WT and STEP KO mice were subjected to MCAO (30 min) and reperfusion (6 h). The STEP peptide mimetic (TAT-STEP-Myc) was administered in a subset of STEP KO mice at the onset of reperfusion (KO + TAT-STEP). (B, C) p38 MAPK phosphorylation and (D, E) COX2 protein level were evaluated by immunoblot analysis of tissue extracts from ipsilateral (B, D) striatum and (C, E) cortex obtained from WT and STEP KO mice. Blots were re-probed with (B, C) anti-p38 MAPK or (D, E) anti-β-tubulin antibody (lower panels). (B-D) Bar diagrams represents mean ± SD (n = 4–6 mice / group). (F, G) PGE_2 level was measured by enzyme immunoassay in the supernatants obtained from ipsilateral striatum and cortex (expressed as ng / mg protein). The corresponding bar diagrams represents mean ± SD (n = 3–4 mice / group). *$p < 0.05$, **$p < 0.001$ and ***$p < 0.0001$ from WT; $^{\#}p < 0.05$, $^{\#\#}p < 0.001$ and $^{\#\#\#}p < 0.001$ from KO.

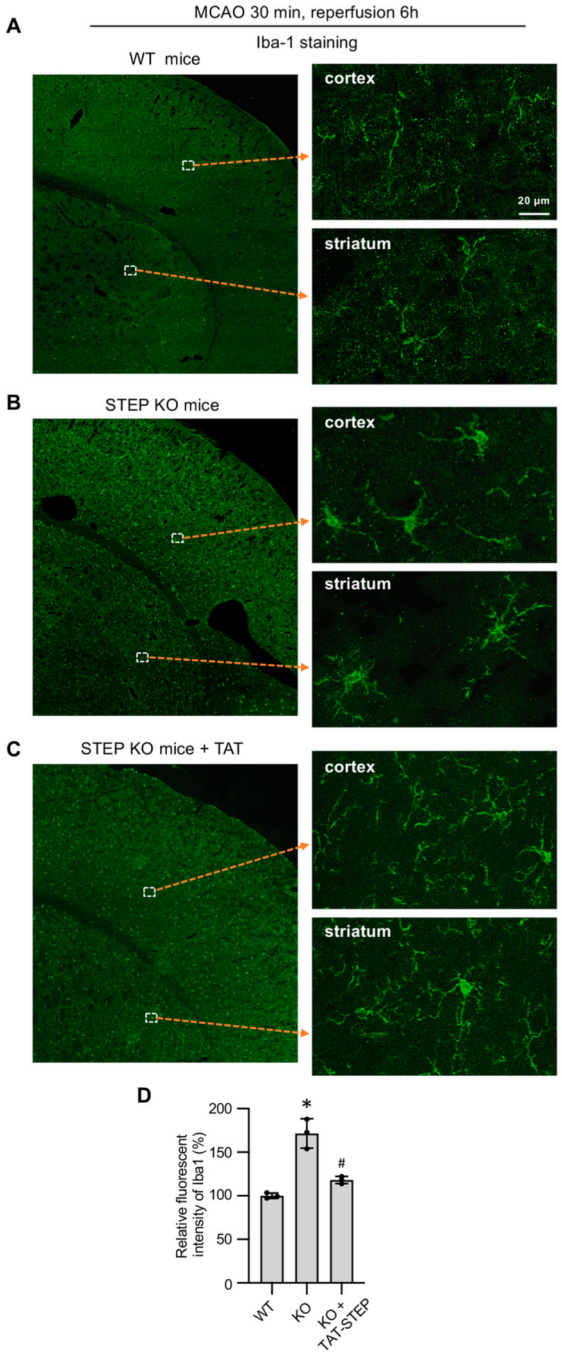

Fig. 5. STEP peptide mimetic attenuates microglial activation in the post-ischemic brain of STEP KO mice.

(A-D) WT and STEP KO mice were subjected to MCAO (30 min) and reperfusion (6 h). In a subset of STEP KO mice, the STEP peptide mimetic (TAT-STEP-Myc) was administered at the onset of reperfusion (KO + TAT-STEP). (A-C) Immunohistochemical staining with anti-Iba-1 antibody show coronal brain sections through cortex and striatum of the ipsilateral hemisphere (left panels). The right panels present higher magnification of the images shown in squares in the left panels. The images in the right panels show changes in microglial morphology (ramified, inactive form or amoeboid, active form), in both the striatum and

cortex. (D) Quantification of immunofluorescent staining intensity of Iba-1 (relative intensity) in the striatum and cortex of the ischemic hemisphere. Values represent mean ± SD (n = 3 mice / group). *$p < 0.001$ from WT and $^{\#}p < 0.001$ from KO.

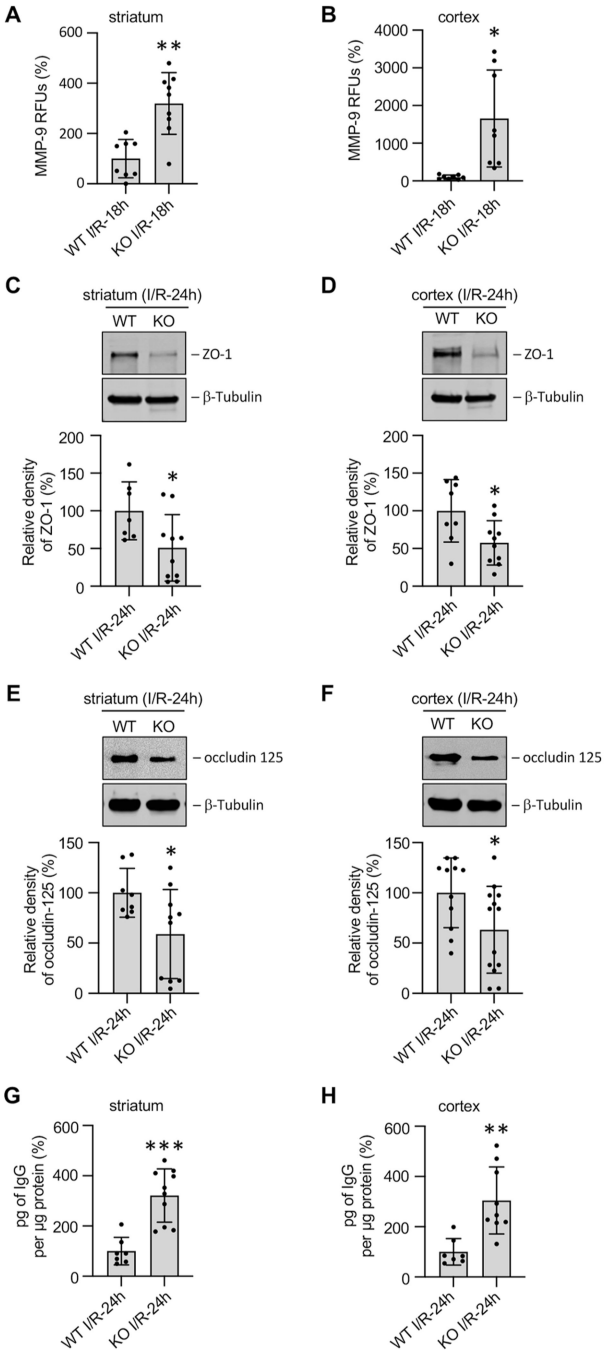

Fig. 6. Ischemic stroke enhances MMP-9 activity, tight-junction protein degradation and BBB permeability in STEP KO mice.

(A, B) MMP-9 activity was measured by a FRET peptide immunoassay in (A) striatum and (B) cortex of WT and STEP KO mice 18 h after post-MCAO reperfusion. Data represents mean ± SD and expressed as relative fluorescent unit (RFU) value for each sample (n = 8–9 mice / group). (C-F) Degradation of tight junction proteins ZO-1 and occludin was evaluated by immunoblot analysis of (C, E) striatal and (D, F) cortical lysates obtained from ipsilateral hemisphere of WT and STEP KO mice, 24 h after post-MCAO reperfusion. Blots were analyzed with (C, D) anti-ZO-1 antibody or (E, F) anti-occludin antibody (upper panels) and

then re-probed with anti- -tubulin antibody (lower panels). Bar diagrams represents mean ± SD (n = 8–12 mice/ group). (G, H) IgG concentration in the (G) striatal and (H) cortical lysates obtained from ipsilateral hemisphere of WT and STEP KO mice 24 h after post-MCAO reperfusion was measured by enzyme immunoassay. Values are represented as mean ± SD (n = 7–10 mice / group). *$p < 0.05$, **$p < 0.001$ and ***$p < 0.001$ from WT.

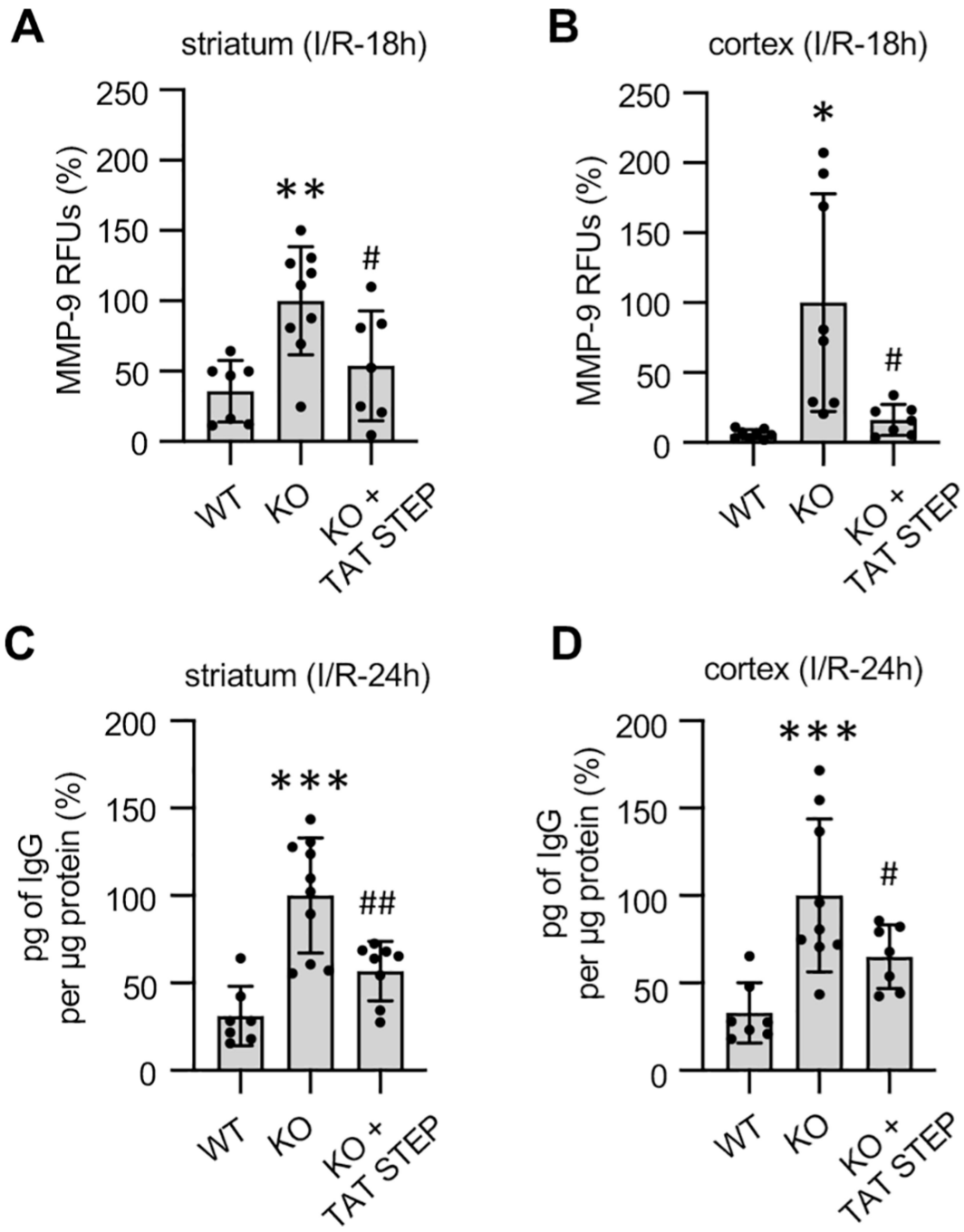

Fig. 7. STEP peptide mimetic attenuates post-ischemic MMP-9 activation, BBB dysfunction, behavioral deficit and brain lesion in STEP KO mice.

(A-D) WT and STEP KO mice were subjected to MCAO for 30 min followed by reperfusion for 18 h or 24 h, and the STEP peptide mimetic (TAT-STEP-Myc) was administered in a subset of STEP KO mice at the onset of reperfusion (KO + TAT-STEP). (A, B) At 18 h of post-MCAO reperfusion, lysates from (A) striatum and (B) cortex were processed for measurement of MMP-9 activity using FRET peptide-based immunoassay. (C, D) At 24 h of post-MCAO reperfusion, lysates from (C) striatum and (D) cortex were processed for measurement of IgG concentration by enzyme immunoassay. Values of MMP-9 activity and

IgG levels are represented as mean ± SD (7–10 mice / group). *$p < 0.05$, **$p < 0.01$ and ***$p < 0.0001$ from WT; $^{\#}p < 0.05$ and $^{\#\#}p < 0.001$ from KO.

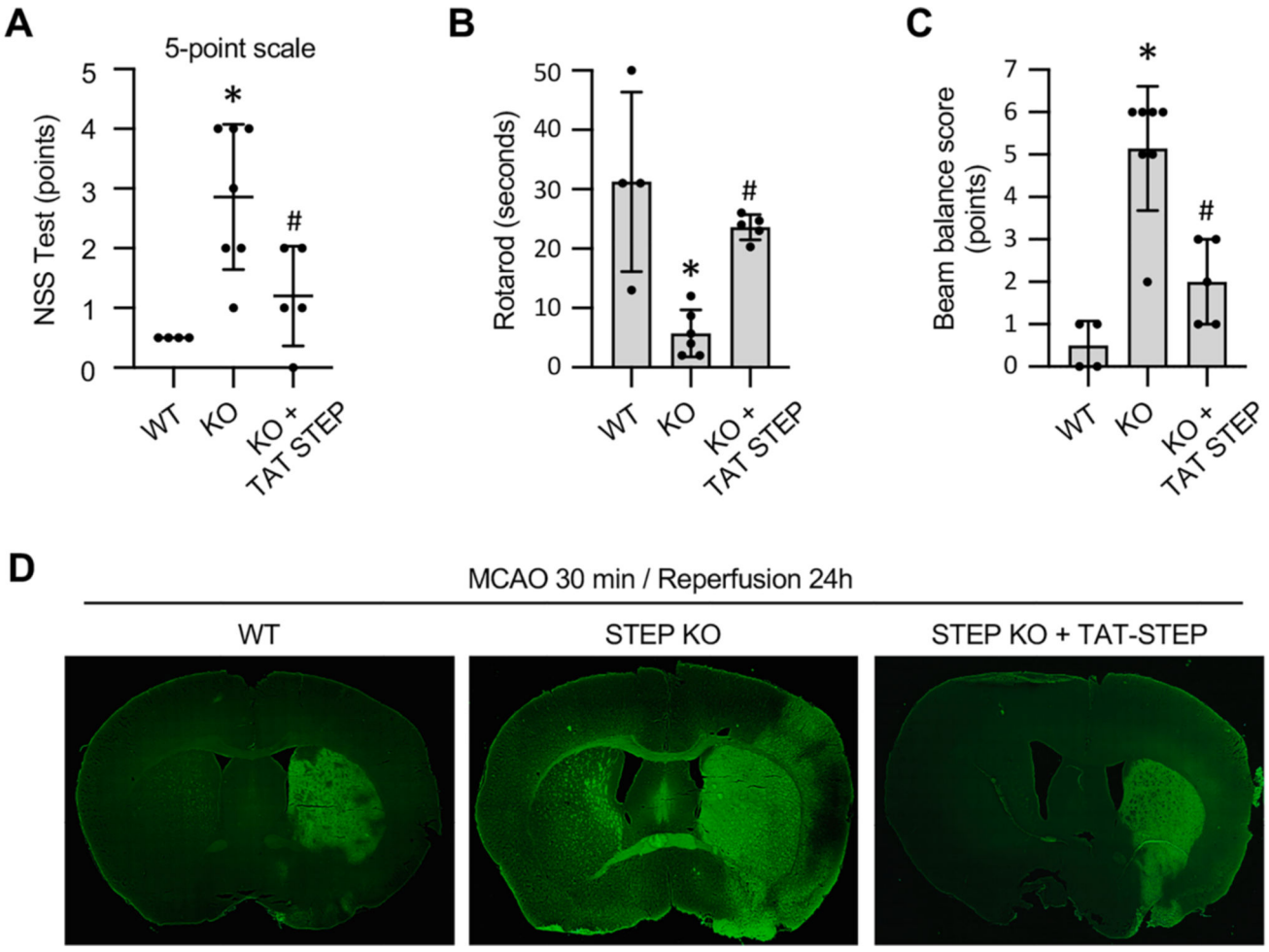

Fig. 8. STEP peptide mimetic attenuates post-ischemic behavioral deficit and brain lesion in STEP KO mice.

(A-D) WT and STEP KO mice were subjected to MCAO for 30 min followed by reperfusion and the STEP peptide mimetic (TAT-STEP-Myc) was administered in a subset of STEP KO mice at the onset of reperfusion (KO + TAT-STEP). At 24 h after reperfusion mice were subjected to behavioral evaluation followed by transcardial perfusion and cryo-sectioning for Fluoro-Jade C staining. (A) Neurological dysfunction was tested using a 5-point neurological severity score; (B) Balance and coordinated alteration of fore- and hind-paw were evaluated using the rotarod; (C) Gait and balance was evaluated using a beam balance task. Bar diagrams represents mean ± SD (n = 4–7 mice/group). *$p < 0.05$ from WT and $^{\#}p < 0.05$ from KO. (D) Representative photomicrographs of coronal brain sections obtained from WT, STEP KO and STEP KO mice treated with the STEP peptide mimetic demonstrating effect of the STEP-peptide mimetic on the progression of ischemic brain damage.

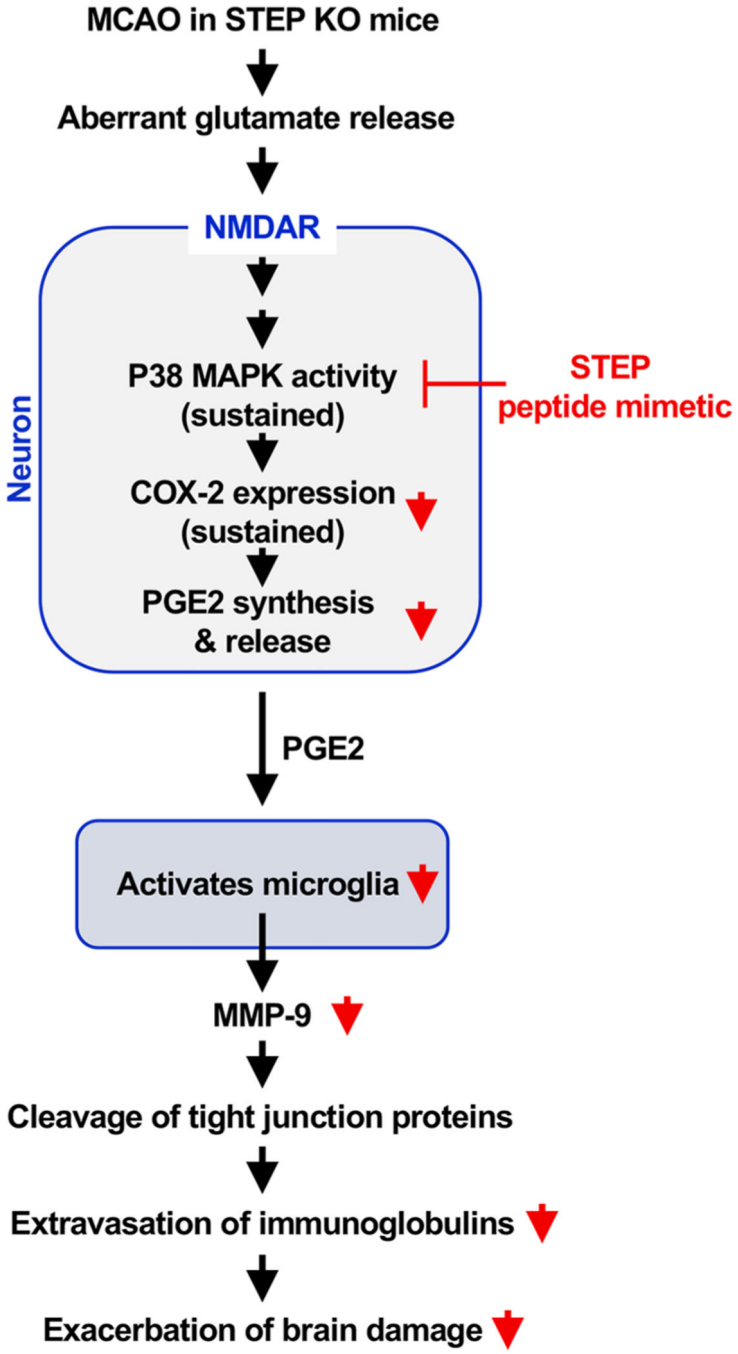

Fig. 9.

A schematic representation of the proposed inflammatory pathway that is involved in exacerbation of ischemic brain injury in the absence of STEP. The arrows in red indicates inhibition of the signaling pathway by the STEP-peptide mimetic. (For interpretation of the references to color in this figure legend, the reader is referred to the web version of this article.)

Table 1

Primary and secondary antibodies used in Western blot (WB) and Immunohistochemistry (IHC).

Antibody	Format	Host	Dilution (WB)	Dilution (IHC)	RRID
Anti-$^{pT123/Y123}$p38	Whole IgG unconjugated	Rabbit	1:1000	1: 100	AB_331762
Anti-$^{pT123/Y123}$p38	Whole IgG unconjugated	Rabbit		1: 100	AB_331765
Anti-p38	unconjugated	Rabbit	1:1000		AB_330731
Anti COX-2	unconjugated	Rabbit	1:2000	1:100	AB_2085144
Anti- β -tubulin	unconjugated	Mouse	1:10,000		AB_477556
Anti-STEP	unconjugated	Mouse	1:2000		AB_10107652
Anti ZO-1	unconjugated	Rabbit	1:1000		AB_2533938
Anti-Occludin	unconjugated	Rabbit	1:1000		AB_2756463
Anti-NeuN	unconjugated	Mouse		1:500	AB_2298772
Anti-Iba1	unconjugated	Rabbit		1:200	AB_839504
Anti-rabbit	peroxidase conjugated	Goat	1:2000		AB_2099233
Anti-rabbit	AlexaFluor-488 conjugated	Goat		1:250	AB_143165
Anti-rabbit	Cy3 conjugated	Goat		1:250	AB_2338690
Anti-mouse	peroxidase conjugated	Goat	1:2000		AB_330924
Anti-mouse	AlexaFluor-488 conjugated	Goat		1:250	AB_2534069